The characterisation of 5-BDBD antagonism of human P2X4 ion channels.

Harry Hickey

A thesis submitted for the degree of

Master of Science by Research in

Biomolecular Science

University of East Anglia

Faculty of Biological Sciences

2019

Words: 22,073

Abstract

The purinergic receptor P2X4 is a ligand-gated, non-selective cation channel, activated by ATP. This receptor is involved in pathophysiological processes including inflammatory pain and cardiac function. Selective inhibition of P2X4 is seen as a possible therapy, however little is known about the limited number of selective antagonists available. This study characterises the activity of 5-BDBD (one such antagonist). There is conflicting evidence for the action of this molecule with one prominent paper suggesting that 5-BDBD is a competitive antagonist and another suggesting that it interacts allosterically. The aims of this study were, to determine the mode of action for 5-BDBD and to identify residues responsible for mediating the effects of 5-BDBD.

When challenging an ATP concentration response curve with various concentrations of 5-BDBD, a reduction in the maximal response (at 20 and 30µM of 5-BDBD) and a decrease in potency (at 10, 20 and 30µM of 5-BDBD) were found. This suggested that 5-BDBD acts allosterically. A scan of the receptor was conducted using 10 amino acid chimeras (P2X4 substituted for aligned insensitive P2X2). This scan used 30µM of ATP and 20µM of 5-BDBD to test for inhibition of the chimeric receptors. There was one chimera (at residues 81-90) which produced a significantly lower inhibition of response than the wildtype ($p=4.8x10^{-4}$). An inhibition of 29.43% was found, compared to the wildtype inhibition of 72.1% with a range for the remaining chimeras of 70.5% to 85.6%. Within this region residue 81 was unique to P2X4 (a phenylalanine residue which was replaced by a histidine residue from P2X2) and when tested, gave a significantly lower inhibition of 42.73% compared to the wild type at 79.2% (P=0.009). This implicates residue 81 with eliciting the inhibitory effect of 5-BDBD on P2X4.

The hope is that these findings can help to determine the binding pocket of 5-BDBD at P2X4, with this residue potentially conferring selectivity for P2X4 over the other receptors in the family.

Table of Contents

List of Figures and Tables

Figures

Tables

List of Abbreviations

AD- Alzheimer's Disease

ADP- Adenosine Diphosphate

ANOVA- Analysis of Variance

ATP- Adenosine Triphosphate

BDNF- Bone-Derived Neurotrophic Factor

BX430- *N*-[2,6-Dibromo-4-(1-methylethyl)phenyl]-*N*'-(3-pyridinyl)urea

Ca^{2+}- Calcium Ion

CaSR- Calcium Sensing Receptor

DAG- Diacylglycerol

DMEM- Dulbecco's Modified Eagle's Media

DMSO- Dimethyl Sulphoxide

DNA- Deoxyribose Nucleic Acid

EC50- Half maximal agonist concentration

ECaC- Epithelial Calcium Channels

E. coli *– Escherichia coli*

eNOS- Endothelial Nitric Oxide Synthase

ER- Endoplasmic Reticulum

FBS- Foetal Bovine Serum

F Ratio- Fluorescence Ratio

GPCR-G-Protein Coupled Receptors

HEK 293- Human Embryonic Kidney 293 cells

HeLa- Henrietta Lacks cells

hP2X4- Human P2X4 receptor

IC50- Half maximal antagonist concentration

KLD- Kinase, Lipase and Dpnl

LB- Loading Buffer

Na^{+}- Sodium Ion

NO- Nitrous Oxide

PBS- Phosphate Buffered Saline

PCR- Polymerase Chain Reaction

PGE2- Prostaglandin E2

PLC- Phopholipase C

PPADS- pyridoxalphosphate-6-azophenyl-2',4'-disulfonic acid

PSB-12062- N-(p-methylphenylsulfonyl)phenoxazine

PTH- Parathyroid Hormone

RA- Rheumatoid Arthritis

RNA- Ribonucleic Acid

RPM- Rotations Per Minute

RTK- Receptor Tyrosine Kinase

SBS- Salt Buffered Saline

SEM- Standard Error of Mean

SR- Sarcoplasmic Reticulum

STC-1- Stanniocalcin-1

TM- Transmembrane

UTP – Uridine Triphosphate

WT- Wildtype

zfP2X4- Zebrafish P2X4 receptor

5-BDBD- 5-(3-Bromophenyl)-1,3-dihydro-2H-Benzofuro[3,2-e]-1,4-diazepin-2-one

Acknowledgements

I am very grateful for the opportunity that has been afforded to me by Dr Sam Fountain as I believe that the environment which he and the other members of his lab has created, has aided me in every aspect of my masters. As my supervisor Dr Fountain has been generous with his time and given any help I have needed throughout this year, providing ideas which have helped to further my project and make it succeed to the extent that it has.

I would also like to thank all of all of the other members of Dr Fountain's labs as they have all helped me to settle in and with any queries I have had along the way. In particular I would like to credit Dr David Richards and Sean Cullum due to them teaching me all of the lab techniques which I would go on to use throughout this project and producing the mutant library which would be very important for my scan of the receptor. Other notable contributions were made by Anna Fortuny-Gomez, Jessica Meades, Dr Mary Gonzalez Montelongo, Mohamed Elday and Dr Neville Ngum.

Finally, I would like to thank my friends and family for the support that they have given me through this year.

Chapter 1: Introduction

1.1 Purinergic Signalling

Purinergic receptors are a family of receptors which can be stimulated by extracellular adenosine triphosphate (ATP) (P2X and P2Y), adenosine diphosphate (ADP) (P2Y) or Adenosine (P1 purinoreceptors). P1 receptors are denoted with the A (P1A1, P1A2a) and the P2 subtype are denoted with a P (P2Y1, P2X3) (Waxham, 2013). P2 receptors are further divided into 2 different phenotypes (P2X and P2Y) (Burnstock, 2014). The P originally stood for purinergic, but it was later found that P2 receptors bound to pyrimidines preferentially over ATP, so now the P is designated to either purine or pyrimidine. P1 receptors can also be stimulated by synthetic adenosine and P2 receptors by synthetic analogues of ATP and UTP.

When Geoffrey Burnstock first proposed the idea of purinergic receptors it was met with some scepticism. This was in some way due to ATP already having an important role as an intracellular energy source and therefore it was believed to be unlikely to act as a neurotransmitter as well (Burnstock, 2006). Over the 1970's and 80's evidence for the 'purinergic theory' mounted and the idea became widely accepted by 1998 when four P1 receptors were cloned and characterised (Ravelic et al, 1998). Purinergic receptors are now known to be widespread in mammalian cells and involved in numerous processes including pain responses, hormone secretion, cardiovascular regulation, cell proliferation, inflammation and apoptosis.

Purinergic receptors can be involved in both short-term and long-term signalling. For an example of short-term signalling, P2Y receptors are involved in the regulation of ion transport for epithelial cells which can have implications for diseases such as Cystic Fibrosis where activation of these receptors can lead to reduced mucous clearance and chronic infection. This occurs due to the increased chloride secretion resulting in thicker mucous. For an example of long-term signalling, several P2Y receptors and P2X5 play a key role in DNA synthesis and cell proliferation which was proven to be the case in mice (Neary et al, 1996) and rat thyroid cells (Ekokoski et al, 2001). More recently the focus has been moved towards purinergic receptors being therapeutic targets for many diseases including epilepsy, atherosclerosis, Alzheimer's, depression and cancer (Burnstock, 2017: Sarti et al, 2018).

P1 receptors are G protein coupled receptors which are endogenously activated by adenosine. There are four receptor subtypes (A_1, A_{2A}, A_{2B} and A_3) which have distinct distributions in mammalian tissues (Abbracchio et al, 2007). These receptors often promote tissue protection and repair via: increased oxygen supply, preconditioning (a form of myocardial protection), modulation of anti-inflammatory effects and stimulation of angiogenesis (Linden, 2005).

P2 receptors are split into two different groups, G-protein coupled receptors (P2Y) and ligand gated ion channels (P2X) with 8 P2Y receptors and 7 P2X receptors currently being recognised in humans. P2Y receptors generally have seven transmembrane domains, an extracellular and an intracellular c-terminal domain. P2X receptors have only two transmembrane domains, a large extracellular domain, an N and a C terminal domain (Burnstock, 1999).

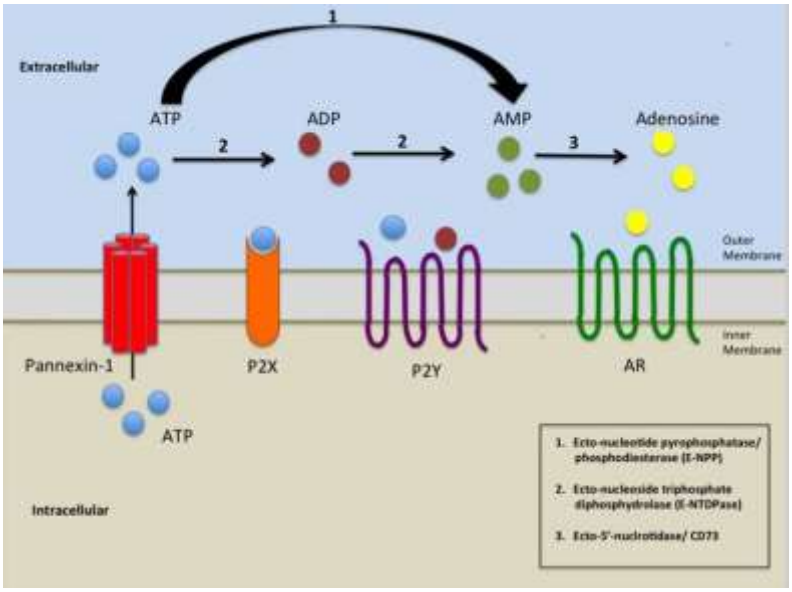

Figure 1.1-Stimulation of purinergic receptors: A diagram showing the release of ATP by a cell, via pannexin-1, to stimulate extracellular P2X and P2Y receptors, the enzymes which break ATP down to its products and the stimulation of P2Y receptors by ADP. Figure taken from Velazquez et al (2014). The AR receptor is shorthand for adenosine receptors (P1 receptors).

Figure 1.1 shows the secretion of ATP by a cell via pannexin-1 which can then stimulate both P2X and P2Y receptors on the cell surface. ATP is broken down to ADP (adenosine diphosphate) by E-NTDPase via cleavage of a single phosphate group from the molecule. ADP can then stimulate P2Y receptors. ADP can also be hydrolysed to produce AMP by E-NPP and then AMP (adenosine monophosphate) by CD73 to produce adenosine which is able to stimulate P1 (AR) receptors (Velazquez et al, 2014).

1.2 P2X Receptors

P2X receptors are a family of non-selective cation channels, within the P2 purinoreceptor group, which are naturally stimulated by ATP. The receptors are each assembled from three subunits ($P2X_{1-7}$) in a homomeric or heteromeric combination (Nicke et al, 1998). P2X7 appears to be the only subunit which is 'unable to make heterotrimeric channels', whilst P2X6 in contrast, very rarely makes homomeric channels (Kaczmarek-Hájek et al, 2012). The subunits have a 'dolphin- like' shape which consists of head, flippers, dorsal fin and tail domains shown in figure 1.2 below. Three subunits join to form a chalice-shaped receptor which has three ATP binding sites formed between two adjacent subunits and using residues from both subunits to interact with the ATP molecule.

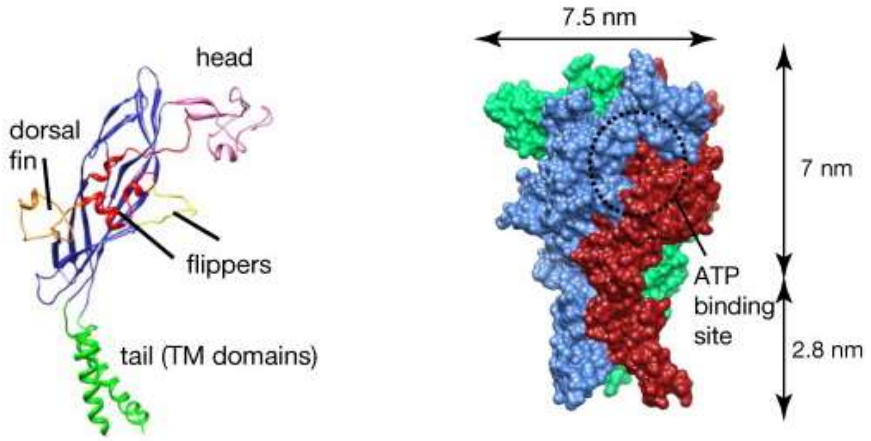

Figure 1.2-P2X monomer and trimer quaternary structure: A diagram showing, with annotations, the characteristics of a P2X monomer signifying the reason for it being referred to as 'dolphin-like' (left). Also, the combination of three of these monomers to produce the fully functional receptor, with lengths of the extracellular and transmembrane/intracellular domain included, as well as an indication of where the ATP binding sites are situated in the trimer (right). Figures taken from work by Young (2010).

Upon ATP binding to the receptor, there is a conformational change in the three subunits which open lateral fenestrations (windows) in the side of the receptor, allowing cations to transverse the cell membrane

The first crystal structure of a P2X receptor was solved by Kawate's group (Kawate et al, 2009), who presented the zebrafish P2X4 in its closed state. This has since been improved upon via the determination of the x-ray structure for both the closed and ATP bound, open channel confirmation for zfP2X. Other P2X receptor structures which have been determined include Gulf Coast tick P2X, human P2X3 (hP2X3) and giant panda P2X7 (Karasawa, 2016: Kasuya et al, 2016), high-resolution structures of the P2X1, P2X2, P2X5 and P2X6 receptors have still not been published.

The number and position of ligand binding sites on P2X monomers was illusive for a long time (Roberts et al, 2006) until these sites were identified for P2X 1-4 using a mutagenesis-based approach which aimed to find the key residues needed for effective binding (Evans et al, 2009: Evans et al 2010). In these studies, the group found that the ligand binding site for zfP2X was generally conserved within the family and that there were several key residues. The residues which they found to be key were Lys68, Lys70, Arg292, and Lys 309 in the P2X primary sequence, which was supported by previous evidence (jiang and Fo, 2000). These were found to be important as mutation of these residues led to a significant reduction in ATP sensitivity. The non-conserved amino acid residues in the sequence are also important as they contribute to the heterogeneity of the receptors. There are three binding sites per functional P2X receptor, with these sites said to be at the interface between two adjacent subunits. This has been corroborated by studies involving radiolabelled ATP (Jiang et al, 2011) which bound to the proposed binding cavity and mutagenesis studies which suggest that residues from the two different subunits are involved in ligand binding (Wilkinson et al, 2006; Rettinger et al, 2007).

1.3 P2X4 Receptors

This study will focus on human P2X4 which was first cloned and characterised from the human brain in 1997 (Garcia-Guzman et al, 1997). This purinergic receptor is found in many tissues including neurons, glandular tissues and endothelial cells. P2X4 is one of the most sensitive purinergic receptors, being stimulated at nanomolar concentrations of ATP, which makes it 1000-fold more sensitive than P2X7 (Burnstock et al, 2011). The P2X4 receptor has been linked to neuropathic and inflammatory pain as well as cardiac function, microglial damage and neuronal development disorders (Yang et al, 2004: Yardley et al, 2013). This has made it a key therapeutic target for these conditions and so research into this receptor has intensified over the last 20 years.

P2X4 is involved in many processes in the body and plays a key role in neuronal function as it is the most widespread P2X receptor in the CNS being expressed in most meurons and glial cells (Bo et al, 2003; Stokes et al, 2017). P2X4 is involved in physiological processes in the CNS such as neurotransmitter modulation and in the hippocampus the presence of P2X4 is believed to contribute to synaptic plasticity (Sim et al, 2006). P2X4 along with GABA receptors may play a role in the regulation of synaptic signalling (Jo et al, 2011). P2X4 is found in an array of epithelial and endothelial cells, performing a wide range of functions. This means that disfunction of P2X4 signalling can cause many different effects in different tissues leading to various pathophysiological processes.

P2X4 is known to regulate the effects of alcohol on microglia (Gofman et al, 2014). Alcohol perturbs many processes in the brain including phagocytosis, cell migration and proliferation (Kumada et al, 2007). In extreme cases alcohol is also known to promote apoptosis in microglia (Sakar et al, 2010). These issues can be attributed to Alcohol-induced expression of P2X4 on microglial cells. A study in 2011 showed that P2X4 knock out mice had a reduction in the detrimental effects of alcohol intake (Wyatt et al, 2014). This receptor mediates its role in neuropathic pain via Brain Derived Neurotropic Factor (BDNF). BDNF is secreted by microglial cells which are activated by ATP. Inhibitors for BDNF have been shown to supress hypersensitivity in several chronic pain models (Masuda et al, 2016) and in contrast the direct injection of BDNF into rats has been shown to cause hypersensitivity, which is where the immune system reacts extremely to a stimulus, causing pain (Lin et al, 2014).

P2X4 is implicated in inflammatory pain as ATP is a pro-inflammatory molecule. This is due to it being a signalling molecule which is involved in triggering the inflammatory cascade. Chronic inflammatory pain arises due to an immune response which is mounted towards a stimulus such as tissue damage, however the pain doesn't subside even after the damaged tissue is repaired (Marchand et al, 2005). The working hypothesis for the role of P2X4 in chronic inflammatory pain is that, ATP released from damaged cells stimulates P2X4 receptors on microglial cells and modulates their function (De Vigrilo et al, 2006: Jarvis et al, 2010). This causes microglia to produce chemokines, cytokines and neurotrophic factors which affect neuronal function, leading to the persistence of the pain sensation (Watkins et al, 2001).

P2X4 receptors are resident on macrophages and when stimulated can cause a Ca^{2+} influx resulting in the cyclooxygenase (COX)-dependent release of Prostaglandin E2 (PGE2) via p38 MAPK phosphorylation. PGE2 is an important cytokine in the inflammatory cascade. In 2010 a group showed that when P2X4 was knocked out in human macrophages, Ca^{2+} influx was significantly reduced (Ullmann et al, 2010). In wild type macrophages, ATP addition resulted in a 3-fold increase in PGE2 production by macrophages, but with P2X4 deficient macrophages the basal rate of PGE2 production was significantly reduced and addition of ATP did not increase PGE2 release. In these P2X4-deficient mice, the receptor was shown to mediate both acute and long-term pain, at least in part due to the release of PGE2. The arrival of macrophages at the site of a wound is followed by the secretion of PGE2 and other cytokines. Initial M1 (pro-inflammatory) macrophages should persist at the site of the wound in the early stages of healing but be replaced by M2 (anti-inflammatory) macrophages once remodelling of the tissue has begun. When this does not happen and there is a prolonged presence of M1 macrophages, there is a prolonged secretion of these pro-inflammatory cytokines resulting in persistent inflammation and pain (Schloss et al, 2018).

P2X4 also plays a role in rheumatoid arthritis (RA) as it promotes inflammation in the joint via activation by ATP. It was shown that targeting the receptor with an antisense RNA led to the suppression of several important pro-inflammatory cytokines (li et al, 2014). This result suggested that Ca^{2+} ion influx through P2X4 is necessary for the production of IL-1β, TNF-a and IL-6 which are key for RA progression. The receptors role in IL-1β secretion was corroborated by a group studying P2X4 activation in osteoarthritis (Fan et al, 2013). Effective P2X4 blockade is therefore a perceived therapy for the chronic inflammatory issues presented in RA.

P2X4 has been implicated in chronic neuropathic pain which arises due to nerve damage caused by trauma, infection or disease which persists long after the event causing the initial damage has healed (Zimmerman et al, 2001). P2X4 was initially shown to be involved in neuropathic pain in 2003 (Tsuda et al, 2003) when a group showed that injection of TNP-ATP (a P2X4 antagonist) into mice who had suffered peripheral nerve injury reduced mechanical allodynia but when PPADS (a non-specific P2X antagonist which doesn't antagonise rat P2X4) was injected, at the same length of time after injury, there was no significant reduction in mechanical allodynia. Allodynia is a form of pain which occurs from normally non-painful stimuli. This and other papers have proven that P2X4 blockade can reverse the effects of allodynia and that when nerve injury occurs there can be a spike in P2X4 expression, causing this chronic neuropathic pain to begin (Inoue et at,2004: Trang and Salter, 2012: Ulmann et al, 2013). These papers suggest that the presence and proliferation of P2X4 in spinal microglia are important for inducing and sustaining neuropathic pain after peripheral nerve injury. There is evidence that interactions between these glia and neurons in the central nervous system are also key in the initiation and maintenance of neuropathic pain (Grace et al, 2011).

A further area of interest for P2X4 research is its role in cardiac function and heart failure. Stimulation of the P2X4R has been shown to activate endothelial nitric oxide synthase

(eNOS), an enzyme that catalyses the production of Nitric Oxide (NO) which has a cardio-protective effect on the heart (Yang et al, 2014). NO elicits its protective effect on the heart due to its role in reducing blood pressure via vasodilation, preventing hypertension which can weaken arteries (leading to myocardial infarctions and strokes). This was shown to be the case with mice that had a loss of function for P2X4, these mice were unable to regulate vascular tone, resulting in cardiovascular disease (Stokes et al, 2011). The link between eNOS and P2X4R was shown to be due to a physical interaction between the receptor and the enzyme which results in the production of NO (Yang et al, 2004). In this same paper Yang remarked that the blockade of P2X4 in the treatment of diseases such as chronic pain could have a detrimental effect on individuals who are under cardiac stress and lead to a higher incidence of heart failure due to the reduced NO production. In terms of a prospective therapy, a targeted treatment which was able to stimulate P2X4 leading to eNOS activation in cardiac myocytes could be beneficial to those at risk of heart failure.

1.4 P2X4 Receptor Pharmacology

P2X4 receptors have been shown to have a high degree of homology between species. Mouse P2X4 has 87% and 94% amino acid sequence homology with its orthologue from human and rat respectively (Jones et al, 2000). Human P2X4 has been shown to be somewhat sensitive to PPADS and slightly sensitive to suramin (two common P2 antagonists) but not to the extent of many other P2X receptors such as P2X1 (Soto, 1999; Garcia-Guzmann, 1997). ATP and several of its derivative including cytidine triphosphate (CTP), 3'-O-(4-Benzoyl)benzoyladenosine 5'-triphosphate (Bz-ATP) and α,β-Methyleneadenosine 5'-triphosphate (α,β-methylene ATP) (He et al, 2003). All of these agonists are non-selective and have a lower potency than ATP. Ivermectin is a positive modulator of P2X4. Upon addition of ivermectin, there is an elevation of the maximum current achieved and a slowing of the deactivation rate for the receptor, when using a patch clamp analysis. These two effects are believed to be mediated by two separate binding sites on the receptor with a high affinity site affecting the maximal current and a lower affinity site affecting deactivation rate (Priel et al, 2004).

P2X4 like the other members in the receptor family is made up of 3 subunits, with the interactions between these subunits forming the binding pocket for agonists. The ATP binding sites are said to be in deep grooves 'outside of the trimer' (Kawate, 2009). This is believed to be the case because, this region contains 10 highly conserved residues and the amino acid composition of this region being compatible with an ATP binding motif (Ennion et al, 2000: Roberts et al, 2004). The binding site takes seven residues (K70, K72, T189, L191, K193, L217 and I232) from dorsal fin and lower body of one subunit and three (N296, R298, and K316) from the head domain and upper body of an adjacent subunit to produce the binding pocket (all numbers are from zfP2X4). Each of these residues has a key role in ATP recognition and placement in the binding pocket. T189, L191 and I232 interact with the adenine moiety and L217 recognises the ribose ring. K70 coordinates the oxygens on the phosphate groups of ATP, K193 and N296 mediate receptor interactions with β phosphate

groups, whilst K72, R298 and L316 are responsible for coordinating the γ-phosphate groups (Chataigneau et al, 2013).

The binding of only one ATP is not sufficient to activate the receptor but does cause a change in the structure, which increases the ease of binding for the second and third ATP (Jiang, et al, 2012). There is evidence however, that the binding of only two ATP molecules may be sufficient activate P2X receptors (Stelmashenko et al, 2012). The binding of three ATP molecules to the three binding pockets of the receptor can activate P2X4, causing a conformational change. Mapping of closed and open state confirmations of P2X receptors show that there is almost no change to the upper domain of the receptor other than a small increase in the pore size at the top of the receptor, although this is still too small to allow the passage of ions through a central pathway via the three vestibules in the ectodomain (Hattori et al, 2012). The head and dorsal fin domains change confirmation slightly also to accommodate the ATP molecule. In the lower body domain however, there is a conformational change to the left and right flipper domains which causes the lower domain to 'flex' outwards, increasing the size of the extracellular vestibule. This flexing provides a pathway for ion influx by creating the lateral fenestrations in the sides of the receptor. In the transmembrane domain (TM), outward flexing of the lower body causes the TM a-helices to expand in a spiral-like fashion increasing the pore diameter and allowing the passage of the cations (Wang et al, 2016).

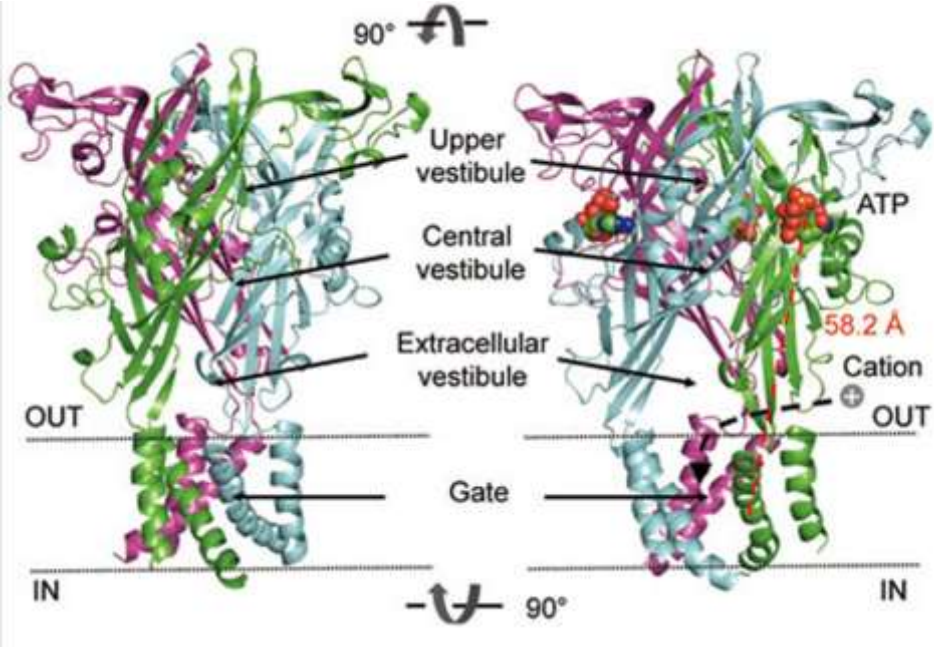

Figure 1.3-Open and closed state zfP2X4 channel: A view of the zfP2X4 channel in closed and ATP-bound open states parallel to the membrane. The main areas of change in the receptor are annotated to show the 'flexing' of the lower body domain and how this increases the size of the extracellular vestibule. The binding site of two ATP molecules is shown as well as how this causes the 'Gate' of this ion channel to open through the separation of the a-helices in the transmembrane domain. Figure taken from Wang et al (2016).

The confirmation of the P2X4 receptor is key to its function. A group showed that the substitution of Tyrosine 315 in the extracellular domain for a cysteine leads to higher pulse pressure. This occurs because another cysteine is introduced to a domain which contains 10 key cysteine residues and may result in the formation of a new disulphide bond, disrupting the channel structure (Stokes et al, 2011). This mutation affects the arterial tone as P2X4 activation causes NO release by endothelial cells (via eNOS) and smooth muscle cell relaxation. Therefore, with this mutation in place there is no NO release and a lack of smooth muscle relaxation, leading to higher pulse pressure (Cragie et al, 2018; Yang et al, 2012).

There are only a few known P2X4 antagonists currently available. These include, paroxetine which is a serotonin reuptake inhibitor which is currently used to treat neuropathic pain (Toulme, 2010). Paroxetine however does not selectively inhibit P2X4 so will have widespread side effects if used solely as an inhibitor for this receptor. Another non-selective inhibitor is TNP-ATP which has potency in the low micromolar range but when looking for an antagonist which could be used as a possible therapeutic aid for P2X4 related diseases a selective antagonist would be preferential. There are several selective candidates currently available such as PSB-12054 which has been shown to have an IC50 value of 189nM and good selectivity for P2X4 over other P2X receptor sub types (Hernandez-Olmos et al, 2012). PSB-12054 conveys its inhibition allosterically. A second selective antagonist is BX-430 which is also allosteric. BX430 was found to have an IC50 of 540nM and is said to be highly selective for P2X4 over other P2X receptors with virtually no effect at these other receptors (Ase et al, 2015; Yatsumura et al, 2016). A third selective P2X4 antagonist is 5-BDBD. There has been debate over the action of 5-BDBD and whether it is an effective selective antagonist for P2X4 as is claimed by the various companies which supply it.

In this project PCR based mutagenesis techniques will be used to identify sites which mediate the inhibitory effects of 5-BDBD on the human P2X4 receptor.

1.5 5-BDBD

5-BDBD (5-(3-Bromophenyl)-1,3-dihydro-2H-Benzofuro[3,2-e]-1,4-diazepin-2-one) is a benzofurodiazepine derivative which is selective for P2X4 at low micromolar concentrations, with one provider claiming that it ‘exhibits no significant antagonist effects at other P2X receptors’ (Tocris, 2019).

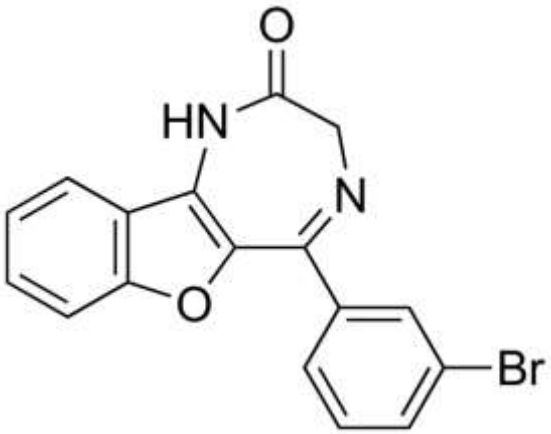

Figure 1.4-5-BDBD structure: The chemical structure of 5-BDBD showing the different groups on the molecule which may interact with the hP2X4R (Sigma Aldrich, 2019).

There is debate as to the action of 5-BDBD due to the conflicting evidence, with some papers stating that it is a completely competitive antagonist and another stating that it is wholly allosteric. The original data which suggested that 5-BDBD acted competitively came from 2013 (Balazs et al, 2013) in which the addition of two different concentrations of 5-BDBD (2μM and 20μM) resulted in a rightward shift of the ATP concentration response curve, without a reduction in the maximal current, which is indicative of a competitive inhibitor. This data has been used by several studies since in order to state the action of 5-BDBD as an antagonist, (Casati et al, 2011; Wu et al, 2011: Bin Ahmad, 2018) with several confirming that it has a similar potency to TNP-ATP. The true nature of 5-BDBD as an antagonist was however disputed in 2017 (Abdelrahman et al, 2017). In this paper the group used a radiolabelled P2X agonist [^{35}S]ATPγS, which the cells were pre-treated with so that the agonist could bind to the receptor before the antagonist was added. They used TNP-ATP, paroxetine and 5-BDBD, aiming to see which of these could displace the radiolabelled ATP. It was shown that TNP-ATP, [^{35}S]ATPγS and 5-BDBD all had a similar potency in this project. TNP-ATP was able to displace the [^{35}S]ATPγS whilst 5-BDBD and paroxetine (a known allosteric inhibitor) were not. 5-BDBD slightly reduced radio-ligand binding at high concentrations, although not significantly. This suggests that 5-BDBD does not competitively inhibit P2X4 because at a high enough concentration a competitive antagonist would displace an agonist due to the dynamic relationship between an agonist and its receptor. This is especially true if the agonist and antagonist have a similar potency. Since TNP-ATP was shown to be able to displace the radiolabelled ATP and 5-BDBD being remarked to have a similar potency to TNP-ATP, this would go to show that 5-BDBD must bind allosterically as the group concluded. There is also evidence from this paper that 5-BDBD is most potent at human P2X4 receptors with its potency being 6-fold less at mouse P2X4 and 10-fold lower for rat. This group does however seem to stand alone in its belief that 5-BDBD acts non-competitively, with much of the literature stating the opposite due to being influenced by the 2013 study.

5-BDBD has been used in several studies already as a means of blocking P2X4 activity such as, 50μM 5-BDBD being applied to gingival keratinocyte as a means to explain the role of the receptor in reactive oxygen species production (Hung et al, 2013). Another study used 10μM

of 5-BDBD to show that P2X4 is the main purinergic receptor which is involved in prechondrogenic condensation. Prechondrogenic condensation is the formation of a cartilaginous template which is replaced by bone in the early stages of embryonic limb development, it is said to be one of the 'most critical processes in skeletal development' (Kwon, 2012).

5-BDBD is believed to be selective for P2X4 with its antagonism being tested at P2X1, P2X3, P2X4, P2X7 and two P2X2 functional splice receptors (a and b) (Coddou et al, 2019). In this study they found that for P2X7 and both P2X2 variants there was no significant inhibition of response when 10μM of 5-BDBD was added for a pre-incubation of 2 minutes. The group did find that 5-BDBD caused a significant reduction in the current amplitude, when performing a patch-clamp assay, for both P2X1 and P2X3 with 12.7% and 35.9% reductions respectively. The inhibition for P2X4 was found to be 83.2%, with the group concluding that 5-BDBD can be used to discriminate between P2X4 and the other receptors used.

Coddou's study was however undertaken using P2X receptors from rats for which 5-BDBD has a lower potency than humans. Another selective P2X4 antagonist (BX430) has also shown species-dependent differences in potency, being a potent antagonist at hP2X4 but having no effect on the mouse and rat orthologues (Ase et al, 2015). There is however no corresponding study for 5-BDBD currently. The only evidence which has been presented to show that there may be species differences was published in 2011 (Vavra et al, 2011). In this study the group applied 5-BDBD to rat brain slices in 3μM and 30μM doses and saw that it failed to inhibit the ATP induced current when performing a patch clamp analysis. In the study they hypothesise that 5-BDBD may not be effective on endogenous heteromeric P2X4 receptors. This may be the case, but It could conversely be due to the species difference.

P2X2 will be used in this project to test the selectivity of 5-BDBD for P2X4 due to it not being significantly inhibited by 5-BDBD for either splice variant tested (Coddou et al, 2019). The selectivity of the inhibitor for P2X4 will be determined by comparing the IC50 value of 5-BDBD for these two receptors in order to understand its potency for each. If P2X2 is significantly less sensitive to 5-BDBD than hP2X4 the aim of this project is to try and locate the sites on hP2X4 which are important for the inhibitory effects of 5-BDBD. This will be attempted by replacing 10 amino acid stretches of the hP2X4 extracellular domain with aligned stretches from P2X2 to make P2X4 chimeric receptors. This should result in there being discrepancies in 5-BDBD efficacy between the different mutants, showing which regions of the receptor may be important in 5-BDBD action.

The PCR-based mutagenesis protocol to be used is similar to that which previously found the ATP binding site for zebrafish P2X4 (Grutter et al, 2013) and human P2X1 (Evans et al, 2007). Another group (Ase et al, 2019) have produced point mutants in several species using a PCR mutagenesis protocol in order to elucidate where BX430 may interact with P2X4. In order to do this, they aligned the sequences for rat, zebrafish and human P2X4 receptors. In this paper, the group identified a single hydrophobic residue (Ile 312) which determined inhibition of P2X4 by BX430, when this residue was substituted with a threonine or glycine residue, sensitivity to BX430 was lost. This also explained the selectivity of BX430 for human P2X4 over the rat and mouse variants as the isoleucine at this position is substituted for a

threonine residue. This paper also suggests that the binding pocket for BX430 is conserved among the P2X family and the presence of the Isoleucine at position 312 allows for inhibition of the receptor. It will be interesting to understand whether 5-BDBD interacts with the receptor in the same region (the potential binding pocket) or at a different site entirely.

When important regions of the receptor are found, smaller changes may be made within these regions in order to find specific residues which may be involved in 5-BDBD action.

1.6 Aims and Hypotheses

In this study the first aim is to characterise the action of 5-BDBD including its mechanism of antagonism at human P2X4, be that via competitive, non-competitive or mixed modal means. This will be attempted by producing ATP d concentration response curves with increasing concentrations of 5-BDBD present. The concentrations that will be tested will be 1µM to 30µM. From the data collected the EC50 value and maximum response achieved at each 5-BDBD concentration can be derived and compared. A competitive antagonist will cause an increase in EC50 value with increasing 5-BDBD concentration and a rightward shift of the ATP concentration response curve. A non-competitive antagonist will cause a reduction in the maximal response achieved with increasing antagonist concentration.

Once the action of 5-BDBD has been determined the next aim will be to find where 5-BDBD may interact with the receptor and discovering whether it has one or multiple binding sites. This will be attempted using PCR based mutagenesis in order to highlight regions on the receptor which may be important for 5-BDBD action and then focusing in on particular regions of interest to see if residues within these regions could be linked to 5-BDBD action.

The final aim will be to present the residues which may be involved in the inhibition of P2X4 by 5-BDBD via showing that mutations to these residues causes a significant reduction in the inhibition of P2X4 by 5-BDBD.

Chapter 2: Materials and Methods

2.1 Tissue Culture

2.1.1 Passaging

In this project 1321N1 cells were used, which is a human astrocytoma cell line that was isolated in 1972 and is often used as a model for neurological diseases. These cells were chosen as they are devoid of endogenous purinergic receptors (Martinez et al, 2016). Therefore, there was no response to ATP for blank (untransfected/parental) 1321N1 cells. This means that when performing transient transfections, there could be confidence that any response above the background level was elicited due to the receptor which had been transfected.

Two distinct 1321N1cell lines were used in this study, the untransfected (parental/blank) cell line and the cell line stably expressing hP2X4. The stable cell line was produced via lentiviral transduction of 1321N1 cells using polybrene reagent (Sigma-Aldrich) which helped to increase the efficiency of gene transfer. The lentiviral particles were produced using co-transfection with 3 plasmids (lentiviral vector containing the transgene, psPAX2 with a CAG promoter and pMD2.G which encodes the envelope glycoprotein). The cells were sorted based on their P2X4 expression using fluorescence activated cell sorting (which identified the mCherry which was also on the plasmid, introduced into the cells) and a cell line highly expressing P2X4 was selected. Clonal cell lines were produced from this initial line based on their Ca^{2+} response and the H8 cell line was selected for this project based on it providing a medial but robust Ca^{2+} response.

Both cell lines were cultured using Dulbecco's Modified Eagles Media (DMEM; Lonza) containing L-glutamine (0.6g/L) which is an essential amino acid for cell growth. 10% (v/v) Foetal Bovine Serum (FBS; HyClone™) which is a source of nutrients for the cells and 1% (v/v) Penicillin/streptomycin (containing 50U/ml of penicillin and 50µg/ml of streptomycin; Gibco™), which was used to reduce the risk of the media becoming infected, were added to 4.5g/L DMEM.

The cells were maintained in ventilated T75 flasks (Thermo Fisher Scientific) which were kept in a 5% CO_2 incubator at 37°C as these were the optimal conditions for cell growth. When 70-80% confluency had been reached, the cells were washed with 3ml of phosphate buffered solution (PBS; Lonza) and then treated with 3 ml of trypsin (0.25% Trypsin/0.2% thylenediaminetetraacetic acid (EDTA) ; Lonza) to sever the cell-cell and cell-plastic adhesions, being returned to the incubator for 5 minutes. The flask was gently tapped to ensure detachment, the detached cells were added to 3ml of media (to stop the enzymatic action of the trypsin) and centrifuged at 1500 rpm for 5 minutes. The supernatant was discarded and the pellet resuspended in 3-5ml of fresh media. The cells were counted using a haemocytometer (to calculate the cells/ml) and a cell solution was made up to the specific density required on the sterile 96 well plates. If the cells were not to be plated, they were passaged, returned to a new T75 flask and placed in the incubator again. These cells were seeded at 50,000 cells/ml. The cells were only passaged up to 20 times before new cells were retrieved from the liquid nitrogen store. All solutions used were pre-warmed to 37°C in a water bath.

2.1.2 Seeding

For non-transfection plates, cells were seeded the night before they were to be used at 35,000 cells/ml. The transfection plates were seeded at 12,500 cells/ml, three days before they were to be used with the transfection happening the day after seeding and there being two days of incubation between transfection and running. This extended period is due to transfection reagents and DNA being toxic to the cells so some cells will die in this stage, meaning it takes longer to reach confluency. Both plate types contained deionised water in the outer wells of the plate to reduce evaporation of the media from the wells containing cells.

2.1.3 Cryopreservation

When there was a surplus of early passage (1-8) cells for either the untransfected or stably transfected lines, these cells were stored in liquid nitrogen for future use. When the excess cells had been passaged and a cell solution produced, this solution was aliquoted into falcon tubes of $1x10^6$ cells. These falcon tubes were centrifuged at 1500 rpm for 5 minutes and the supernatant was discarded. The resulting pellet was resuspended in 900µl of media containing 70% DMEM and 30% FBS. This solution was transferred to a cryovial and had 100µl of sterile 100% DMSO added to it, which prevented crystals from forming intracellularly when freezing. This produced a final solution which was $1x10^6$ cells/ml. The vials were moved to a MrFrosty™ (Thermo Scientific) to slowly regulate temperature reduction and stored at -80°C for 24 hours. After this period the vials were moved to the Liquid nitrogen store for long term storage.

When the cells were needed, they were removed from the liquid nitrogen store and thawed in a water bath at 37°C until nearly all of the solution had thawed. The solution was then quickly diluted in 4ml of fresh media and centrifuged at 1500 rpm for 5 minutes. The supernatant was decanted and the pellet resuspended in 1ml of media. The new cell solution was then added to a T25 flask containing 4ml of fresh media. The cells were placed in a 5% CO_2 incubator at 37°C for 24-48 hours, depending on growth rates and when they approached confluency, the cells were passaged in the fashion described in 2.1.1 and either seeded in a T75 or on a 96-well plate.

2.1.4 Salt Buffered Saline and Loading Buffer preparation

Salt buffered saline (SBS) was prepared in deionised water and contained the following in the given concentrations: sodium chloride (NaCl) 130mM, potassium chloride (KCl) 5mM, D-(+)-glucose 8mM, HEPES (4-(2-hydroxyethyl)-1-piperazineethanesulfonic acid; Fisher Scientific) 10mM, magnesium chloride ($MgCl_2$) 1.2 mM and calcium chloride ($CaCl_2$) 1.5mM. The solution was titrated to pH 7.4 in 1L of SBS using 10mM sodium hydroxide (NaOH).

To produce loading buffer (LB), pluronic acid was added to 200ml of SBS (0.01% (w/v)). Pluronic acid helps to stabilise the cell membrane preventing shearing upon Fura-2 entry into the cells, reducing losses in cell viability (Tharmalingam et al, 2008). The supplier of all chemicals was Sigma-Aldrich if it is not stated to the contrary.

2.1.5 Plate preparation

Stably expressing cells were seeded at 35,000 cells/well and incubated at 37°C in 5% CO_2 for 24 hours before running.

Transiently transfected (parental) cells were seeded at 12,500 cells/well, being incubated for 96 hours (with transfection after 24 hours).

The parental cell line was seeded at a lower density as transfection is made harder when cells approach confluency and this allowed cells to have a longer period of growth to recover after transfection.

To prepare for the Flexstation, the media in the wells was removed and the cells were washed with SBS, to remove dead cells and any remaining media. Loading buffer with 2µM Fura-2 (Abcam) is then added to the wells (200µl per well) and incubated for one hour, to allow time for Fura-2 to enter the cells and have its AM domain cleaved.

The loading buffer was removed, the cells were washed with 200µl of SBS twice and finally 199µl (5-BDBD protocol) or 200µl (non 5-BDBD protocol) of SBS was added to the wells. If there was to be 5-BDBD used, 1µl of 5-BDBD at a given concentration (produced by diluting a frozen 10mM stock of 5-BDBD made by dissolving powdered 5-BDBD in 100% DMSO) or 100% DMSO was added to each well and the plate was incubated for 30 minutes before running. This resulted in a final 5-BDBD or DMSO concentration of 0.05% in each well. If 5-BDBD was not in the protocol, the plate could be run immediately. The plates were wrapped in tin foil for incubations and all work is to be done in the dark, in order to protect Fura-2 from photo-bleaching.

ATP was made by dissolving powdered ATP in SBS to make a 10mM stock. A new stock must be made for each plate which is run, this is to reduce the chance of a mistake on one plate being carried over to further plates. From the stock solution the highest concentrations to be used were produced by diluting the stock in SBS. From these the rest of the concentrations used on the plate were produced by serial dilution. If one ATP concentration was to be used for the whole plate, a stock solution was produced from the 10mM stock by diluting in SBS. 70-80µl of the relevant ATP concentrations were pipetted into a 96-well round bottom plate in the corresponding position of the well which they were to be added to on the flat bottom plate containing the cells. All solutions were pre-warmed to 37°C in a 5% CO_2 incubator.

2.2 Transient Transfection of P2X4 Protocol

Transfection is a process by which exogenous DNA is introduced into a cell and incorporated into its genome. In this study the exogenous DNA encoded the hP2X4R gene and gave the parental cell line the ability to express P2X4.

The full transfection protocol took four days from seeding to running the plate. On the first day 12,500 cells were seeded per well after being passaged and counted. The plate was left in a 5% CO_2 incubator over night at 37°C. On day two, the media in the wells was removed and replaced with 200µl of fresh media, this was to remove dead cells which failed to adhere to the bottom of the well. Stock solutions of DNA and Lipofectamine 2000 were made by diluting both in optimem media (Thermo Fisher Scientific) in order to reach a

concentration twice that of what was needed on the plate (300ng/well of DNA and 0.5µl/well of lipofectamine on the plate). The DNA and Lipofectamine 2000 stock solutions were combined to produce a master mix (halving their concentrations). The master mix was incubated at room temperature for 5 minutes to allow the Lipofectamine to bind to the DNA. 10µl of the master mix was added to each well and the plate was returned to the incubator for two further days. The plate was run using the method for 5-BDBD addition.

2.3 DNA Extraction

1-2µl of a frozen glycerol stock of *E. coli* was pipetted onto a 20ml agar plate (fisher Scientific) made with 20µl of Ampicillin (100 µg/ml; Sigma Aldrich) included (which the *E. Coli* had a resistance gene for). The agar and ampicillin were combined and swirled for 2-3 minutes to ensure homogeneity of ampicillin in the agar before use. The plates were incubated for 16 hours at 37°C in a 5% CO_2 incubator. One colony was chosen from the agar plate and place into a universal tube containing 12ml of LB broth (Fisher Scientific) and 0.001% Ampicillin (v/v). The universal tubes were incubated for 16 hours in a rotating incubator (225 rpm) to prevent the cells from sedimenting at the bottom of the tube. The universal tubes were centrifuged at 2000 rpm for 20 minutes, the cells were ligated and the DNA collected and purified by following the instructions for the omega ENZA mini-prep kit (omega bio tek). The extracted DNA was tested for purity and concentration using a Nanodrop 2000 spectrophotometer (Thermo Fisher) before use.

2.4 Mutagenesis

All mutagenesis steps were performed using the Q5® Site-Directed Mutagenesis Kit™ (New England biolabs).

Both LB broth and LB Agar were produced by 40g of powdered Agar (Fisher Scientific and 20g of powdered LB broth (Fisher Scientific) respectively being dissolved in 1L of deionised water and autoclaved to ensure homogeneity.

2.4.1 Designing Primers

All primers used within this project for the production of chimeras, were produced using the New England BioLabs online design software, NEBaseChanger™ (NEBaseChanger, 2019). The primers were purchased from Thermo Fisher Scientific and came premade in 10µM stocks. These Primers were stored at -20°C until they were to be used.

The primers produced using this method and utilised in this project are stated below:

Name (F/R)	Oligo (Uppercase = target-specific primer)	Len	% GC	Tm	Ta *
Q5SDM_6/29/2019_F	gtggcggattatgtgATACCAGCTCAGGAGGAA	33	52	62°C	60°C
Q5SDM_6/29/2019_R	atcccagatccggtgTCCAAGTTTAGAAGTGTTGG	35	49	59°C	

* Ta denoted the recommended annealing temperature that was to be used in the PCR step.

2.4.2 PCR

Firstly, the DNA was amplified using polymerase chain reaction (PCR) which cycled different temperatures for differing periods which allowed the primers to insert the chimeric DNA into the wildtype plasmid and for the amplification of this plasmid. Each reaction was performed by combining 1µl of wildtype P2X4 plasmid (20ng/µl), 1.25µl of both the forward and reverse primers (10µM stock solutions), 9µl of nuclease-free water and 12.5µl of Q5 hot start high-fidelity master mix in a PCR tube.

Table 1- PCR Methods: The stages involved in the PCR process with temperatures and the time each step takes delineated. There were 25 cycles in the amplification steps which followed a cycle of denaturation, annealing and then extension moving downwards. There were two variables which were specific to this project the annealing temperature could change within this range based on the size of the primers and secondly the extension time was calculated by 30 seconds multiplied by the number of Kilobases of the final PCR product.

Step	Temperature	Time
initial		30
Denaturation	98°C	seconds
		10
	98°C	seconds
25 cycles		20
	50-60°C	seconds
	72°C	5 minutes
Final Extension	72°C	2 minutes
Hold	4°C	∞

The PCR was performed in a thermocycler (Verti) and the PCR product was stored at -20°C until it was to be used in the KLD reaction.

2.4.3 Kinase, Lipase and DpnI Reaction

The Kinase, Lipase and DpnI (KLD) reaction took 1 µl of the PCR product and added 5µl of KLD reaction buffer, 1µl KLD enzyme mix and 3µl of nuclease free water in a fresh Eppendorf tube. The solution was incubated at room temperature for 30 minutes.

2.4.4 Transformation

5µl of the KLD reaction solution was added to 50µl of chemically competent *E. coli* cells, which were thawed on ice for 5 minutes prior to KLD solution addition. The cells were incubated for 30 minutes on ice, then heat shocked at 42°C for 30 seconds (to induce competency and allow the plasmid to enter the cells) and incubated on ice for 5 minutes. 450µl of super optimal broth with catabolite repression (SOC) media was added to the cells and they were incubated in a rotating incubator (125rpm) at 37°C for 1 hour.

Finally, 50 and 200µl of the solution was pipetted onto agar selection plates and incubated at 37°C in 5% CO_2 for 16 hours.

2.4.5 DNA Isolation and Testing

A colony was selected from the agar plate and added to a universal tube containing 12ml of LB broth and 0.1% ampicillin (v/v). The tube was incubated at 37°C in a rotating incubator (225 rpm) for 16 hours. The DNA was extracted following the omega ENZA mini-prep kit and Nanodrop tested for purity. The DNA was then diluted to 100ng/µl and 5µl was sent to Source Bioscience for sequence analysis. When the sequence returned it is checked using Clustal Omega (EBI) and Sequence Manipulation Suite (Bioinformatics.org) to ensure that the correct mutation had been made and that there were no other mutations which had occurred in the amino acid code. Glycerol stocks of the E. coli were produced by taking 1.2ml from the overnight culture in the universal tube and adding it to 300µl of glycerol in a 1.5ml Eppendorf tube. These stocks were stored at -20°C until needed.

2.5 Flexstation Protocols

In this study a Flexstation III was used running on the program SoftMax Pro. The Flexstation used this program in order to present the Fura-2 fluorescence graphically over the period of observation for each well (250 seconds). The Flexstation pipetted 50µl of agonist into each well after 20 seconds of the assay and the change in intracellular free Ca^{2+} concentration was recorded for the remainder of the time. The change in intracellular Ca^{2+} was signified by a change in Fura-2 fluorescence ratio (340:380nm).

Fura-2AM contains an acetoxymethyl ester group attached which allows the molecule to enter the cell. Once inside the cell the AM group is cleaved by cellular esterases, rendering the Fura-2 unable to exit the cell. Fura-2 binds to intracellular free Ca^{2+} and fluoresces at 3 distinct wavelengths: 510nm, 340nm and 380nm with 510nm fluorescence being constant (MacDermott et al, 1994). When not bound to Ca^{2+} Fura-2 fluoresces at 380nm but when it is bound to Ca^{2+} it fluoresces at 340nM. The ratio of bound to non-bound Fura-2 can be used to quantify the concentration of intracellular Ca^{2+} as Fura-2 naturally binds to free intracellular Ca^{2+} with a high affinity (Paredes et al, 2008). This meant that the concentration of Ca^{2+} bound Fura-2 was a good indicator for the concentration of intracellular Ca^{2+} in general. The concentration of intracellular Ca^{2+} changing was therefore used as an indicator for cation movement in general as P2X4 is a non-selective cation channel. This ratio of 340nm to 380nm was shown on the SoftMax program as an 'F ratio' which allowed for comparison between different conditions (such as changes in ATP or 5-BDBD concentration).

2.6 Data Analysis

The Data was collected by the SoftMax Pro program in the form of the peak F ratio achieved in each assay and exported to excel. The data had the blank response removed, this was the basal response which was caused by small fluctuation in F ratio, resulting from the dynamic relationship between Fura-2 and the intracellular Ca^{2+} before ATP addition. The blank response was calculated from 3 or more wells on each plate which contained cells at the same density as the rest of the plate but had 50 µl of SBS added to them rather than 50µl of agonist. The data was then normalised to the concentration giving maximal response or a control on each plate. An average of the repeats on each plate, for each concentration, are

taken and the data from the five plates are amalgamated in Origin student pro 2018 software (Origin Labs).

All data was presented as a mean with standard error and on each plate there was at least a triplicate for every data point. The n number refers to the number of individual plates which were repeated for each data point on a graph.

Many of the graphs were fitted with a concentration response curve using the Hill1 equation which aided in the derivation of EC50 (agonist concentration needed for a half maximal response) and IC50 (antagonist concentration needed for a half maximal response reduction) values. The Hill equation was used to show the degree of cooperation between a receptor and its ligand, allowing the quantification of this interaction via production of the hill coefficient. In this project a modified version was used (called Hill1 on origin labs) where Vmax is replaced by Start + (End – Start) in the equation. This provides the equation with offset and fixes the n number which is variable in the standard Hill equation.

Hill1: $$y = START + (END - START)\frac{x^n}{k^n + x^n}$$

In this equation, k denotes the Michaelis constant and n denotes the number of cooperative sites.

T-tests or one-way ANOVA statistical analyses were performed if the data was normally distributed using a Shapiro-Wilk test and had equal variance using a Levene test. For data sets which were not normally distributed or had unequal variance a Kruskal-Wallis ANOVA was used followed by a post-hoc analysis.

Chapter 3: Results

3.1 Transfection Protocol

When trying to find an efficient protocol for transfecting 1321N1 cells there were four candidate transfection reagents in contention, three of which had been previously shown to provide adequate transfection (Marucci et al, 2011). The transfection reagents tested were FuGene, Polyfect, Lipofectamine and X-treme gene. Each reagent was tested at a range of DNA and reagent concentrations to try and find the optimal conditions for transfection using that specific reagent before comparisons between them were made.

Polyfect and FuGene were eliminated from contention due to the inconsistency of transfection and both giving a low response when stimulated with maximum ATP (30µM).

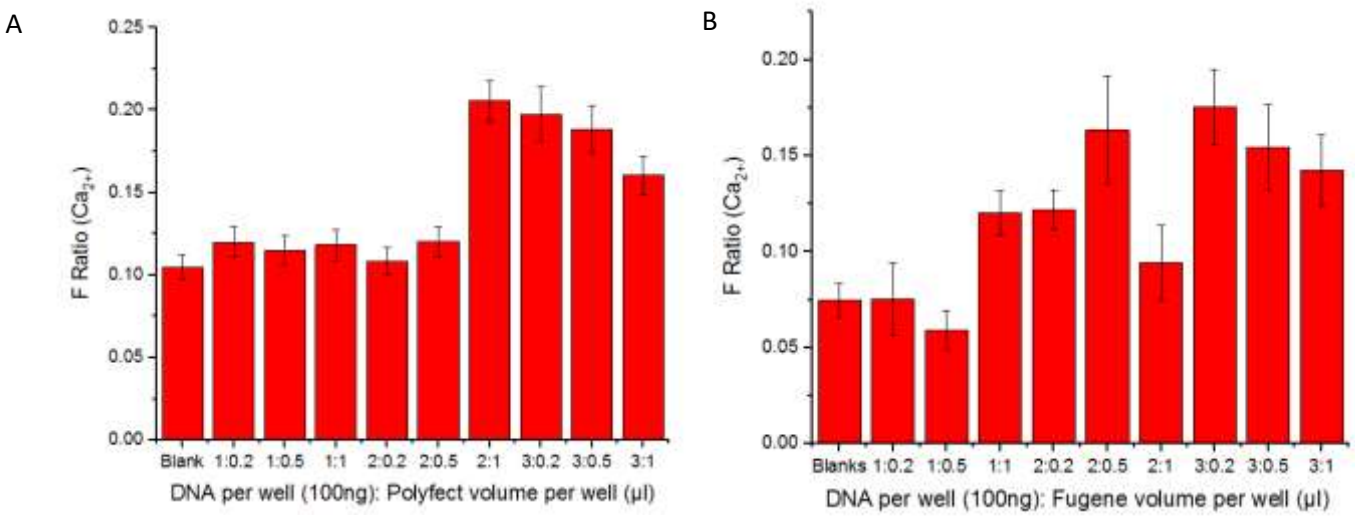

Figure 3.1-Polyfect and FuGene transfection reagent scan: Two graphs showing the peak response elicited by 30µM ATP for each tested combination of transfection reagent and DNA. The left diagram (A) shows the data for Polyfect and the right (B) shows FuGene. Both graphs have the blank response included for reference (n=3). The x axis shows a ratio of DNA to the reagent.

Figure 3.1 shows that Polyfect and FuGene were both unsuitable to be used as the transfection reagent for this study as they both failed to elicit a response which was significantly different from the background (blank). The highest F ratio achieved was 0.21 for Polyfect and 0.17 for FuGene which would not be sufficient when undertaking the PCR-based mutagenesis studies. This was due to the need for a robust response which could provide a discernible difference between inhibition with 5-BDBD and a non-inhibited response once the background had been removed.

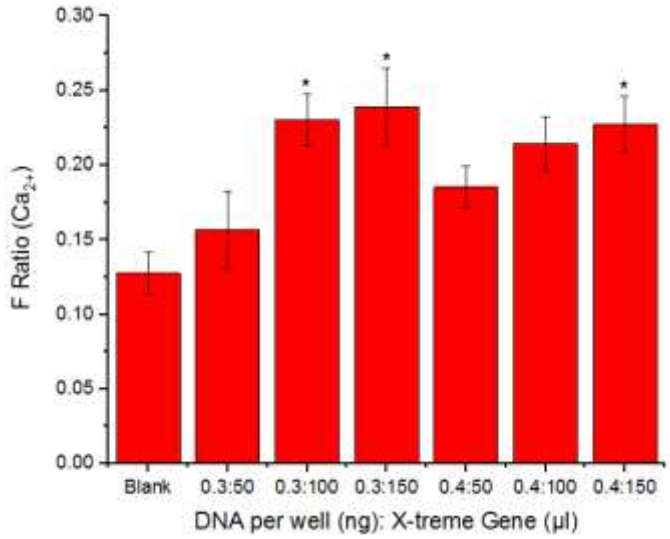

Figure 3.2-X-treme Gene transfection reagent scan: A graph showing the calcium response elicited by 30µM ATP at several different conditions for X-treme Gene. Those concentrations which produced a response significantly different ($p<0.05$) from the control are marked with an asterisk (n=3). The x axis shows a ratio of DNA to transfection reagent.

The next reagent tested was X-treme Gene which was more successful, having three separate concentrations which were significantly different from the control. The best of the concentrations tested for this reagent was 0.3µL of reagent and 150ng per well of DNA which gave an F ratio response of 0.24 which was higher than for the previous two reagents but relatively still low.

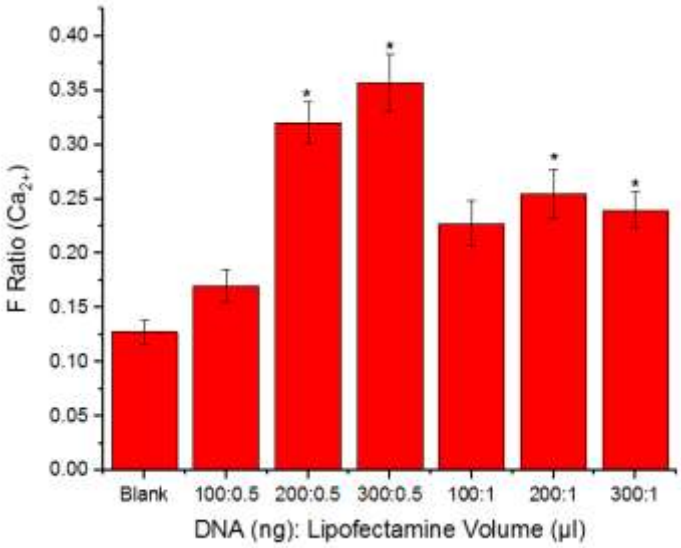

Figure 3.3-Lipofectamine transfection reagent scan: A graph showing the response elicited by 30µM ATP on cells transfected with varying ratios of DNA to Lipofectamine transfection reagent. The ratios which produced a response significantly different ($p<0.05$) from the control were denoted with an asterisk (n=3).

The final reagent tested was Lipofectamine which produced four conditions that were significantly higher than the control response. Of these the largest response was elicited by 300ng of DNA and 0.5µl of Lipofectamine per well. The response on average for this condition was 0.36 which was higher than 0.17, 0.21 and 0.24 achieved for the other

reagents. Lipofectamine at this concentration ratio was therefore chosen for the proceeding transfection protocol.

3.2 ATP Concentration Response

An ATP concentration response curve was produced for both hP2X4 and hP2X2. Both receptors were expressed in stably transfected 1321N1 cell lines.

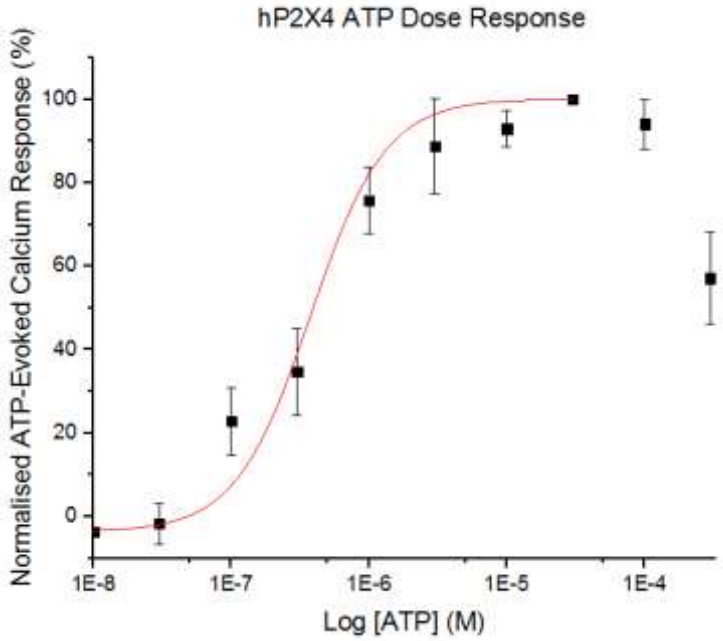

Figure 3.4-hP2X4 ATP concentration response curve: A graph showing the normalised peak response of human P2X4 to ATP concentrations between 10nM and 300µM. The data is normalised to the maximal ATP concentration. The curve has been fitted with the Hill1 equation in order to determine an EC50 (n=5).

Figure 3.4 shows that the data follows a sigmoidal fit with the curve plateauing at a maximal concentration of 30µM. Using the Hill equation an EC50 value of 379.80 ± 98.96nM was derived from the graph. It was however said to be 7.4 ± 0.5 µM in the literature (Soto et al, 1996; Garcia-Guzman et al, 1997) which was significantly different from the potency found in this assay. For concentrations higher than 30µM there was a reduction in response measured by the Flexstation. This was due to desensitisation of the receptor to ATP at high concentrations which is common for P2X4.

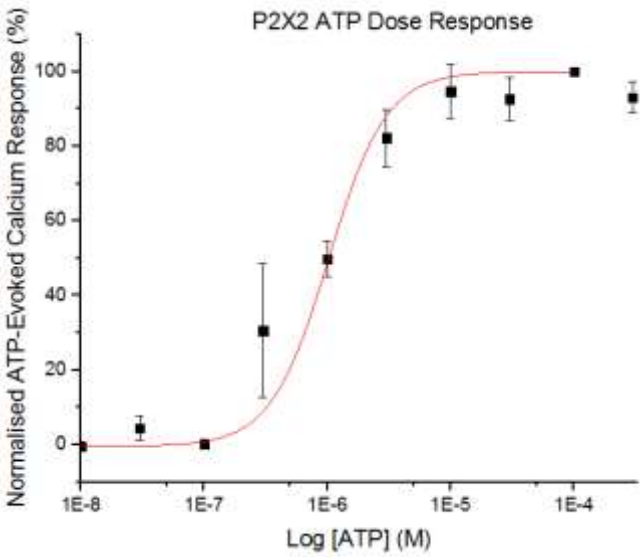

Figure 3.5-hP2X2 ATP concentration response curve: A graph showing the normalised peak response of hP2X2 stably expressed in 1321N1 cells. The receptors were stimulated with ATP concentrations between 10nM and 300 µM. The data was normalised to the maximal response and had a sigmoidal fit added to it using the Hill1 equation in origin labs (n=5).

Figure 3.5 also shows a common sigmoidal fit with a plateau at the lowest and highest concentrations and a characteristic rapid increase between 100nM and 3µM. The EC50 derived from this graph was 1µM, which was in line with that previously found for P2X2 (North et al, 2009). When comparing the EC50 values for the five repeats of P2X2 and P2X4 the two receptors were shown to be significantly different, with a kruskal-wallis post-hoc analysis showing that P2X2 had a significantly higher EC50 value. Another difference between the two receptors was the lack of desensitisation at P2X2 with the highest ATP concentrations not causing a reduction in response like was seen for P2X4. In figure 3.5 there was a high degree of error at 300nM which is common in the rapidly increasing phase of a sigmoidal curve due to the variation in EC50 position between the repeats meaning that concentrations within this phase can have largely different normalized responses.

3.3 IC50 Curve Derivation

Next an IC50 curve was derived for each of the receptors (P2X2 and P2X4) to determine what concentration of 5-BDBD causes a half maximal reduction in the receptor response.

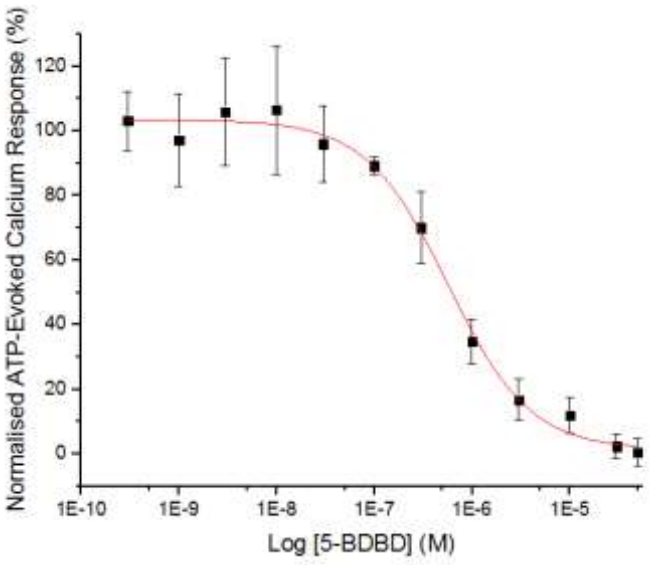

Figure 3.6-hP2X4 IC50 curve: A graph showing the response of P2X4 expressing cells to increasing concentrations of 5-BDBD between 300pM and 50µM when stimulated with 500nM ATP. The graph is fit with a Hill1 equation in order to find the IC50 value. The points are all plotted with their standard error (n=5).

In figure 3.6 you can see that with increasing concentrations of 5-BDBD after 30nM there was a decrease in the normalised response of P2X4 to ATP. This reduction begins to plateau at 10 µM. At the low nanomolar concentrations of 5-BDBD there is a plateau at around 100% of the normalised response. The IC50 value found for this data set was at 873.9nM which would suggest that it was a fairly potent agonist of P2X4.

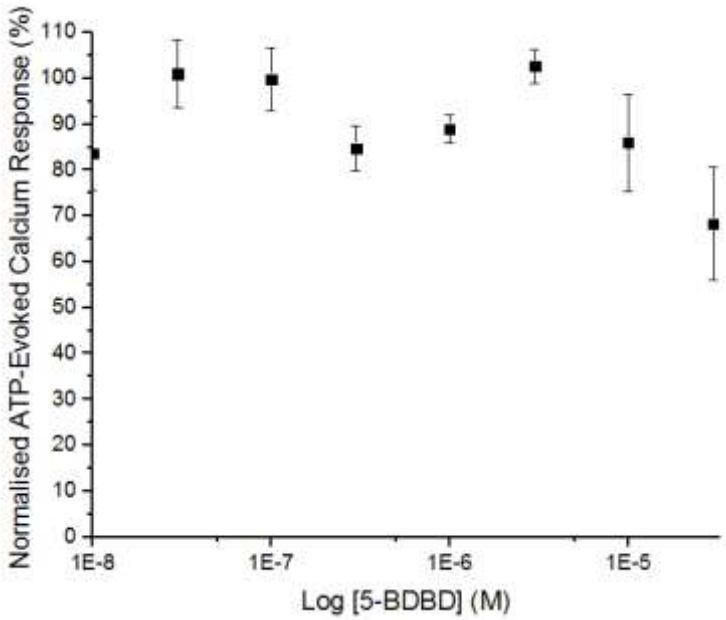

Figure 3.7-hP2X2 IC50 curve: A curve showing the change in response of P2X2 receptors in the presence of increasing 5-BDBD concentrations from 10nM to 30µM. The cells were stimulated with 1µM ATP. The points are all depicted with standard error (n=5).

Figure 3.7 shows that with increasing concentrations of 5-BDBD there was no pattern signifying a reduction in ATP response. This was confirmed when performing a Kruskal-Wallis non-parametric analysis on the data which showed that no concentration of 5-BDBD used was significantly different from another concentration in the study. Analysis also showed that there was no significant difference between ATP and any of the concentrations tested for. There was a reduction in response at 30µM, but it was not statistically significant, possibly due to the high error at this concentration. This lack of response reduction differs from hP2X4 as the response was approximately 11.9% of maximal response at 10µM compared to 86.3% for P2X2. An attempt was made to fit a Hill equation to the graph but an IC50 value for the data set was unable to be determined.

3.4 The effect of 5-BDBD on a hP2X4 trace

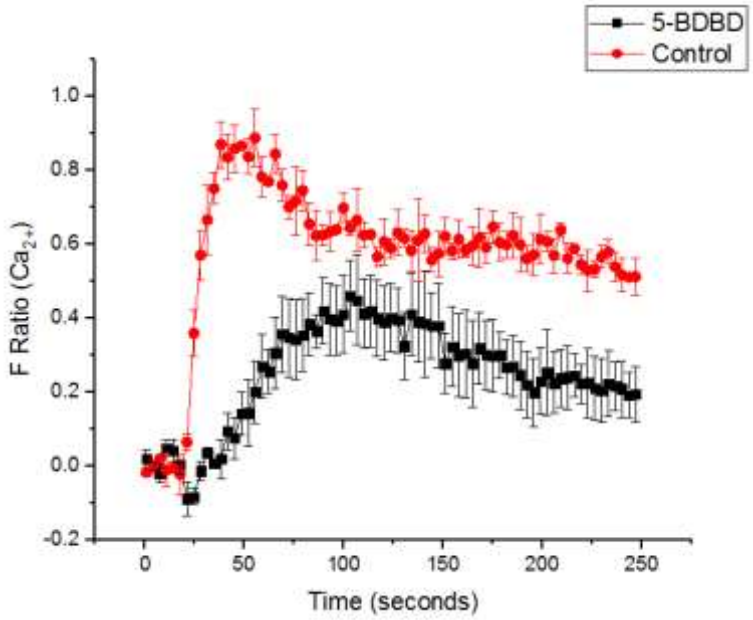

Figure 3.8-20µM 5-BDBD trace for hP2X4: A graph of representative traces to show the difference between a Flexstation trace without 5-BDBD being added to the cells (red) and when 20µM is present (black). Each of the traces had 30µM of ATP added after 20 seconds of the assay. The stably transfected hP2X4 cell line was used (n=1).

Figure 3.8 above shows a representative ATP concentration response trace with 30µM of ATP added in the presence and absence of 5-BDBD (20µM). This gives a clear indication of the inhibitory ability of 5-BDBD due to its reduction of the peak F ratio achieved and the change in shape of the trace in its presence. The peak value achieved on a trace was what was analysed to signify any changes which have occurred when changing ATP or 5-BDBD concentration in an assay. It can be seen by the change in shape of the trace that 5-BDBD not only reduces the maximum response seen (a reduction to 47.35% of the red trace), but also increases the time taken to reach this point after ATP addition.

3.5 5-BDBD Response Curves

A

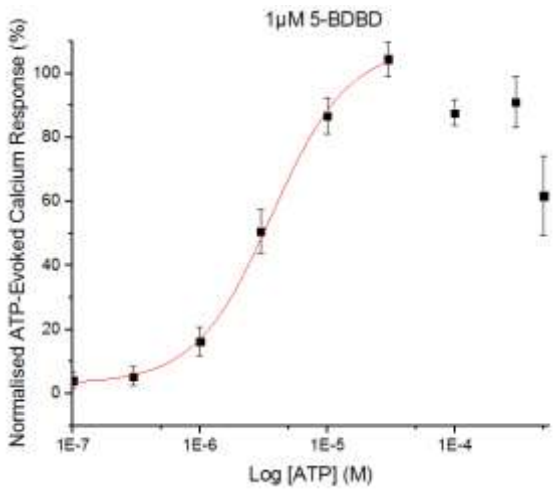

B

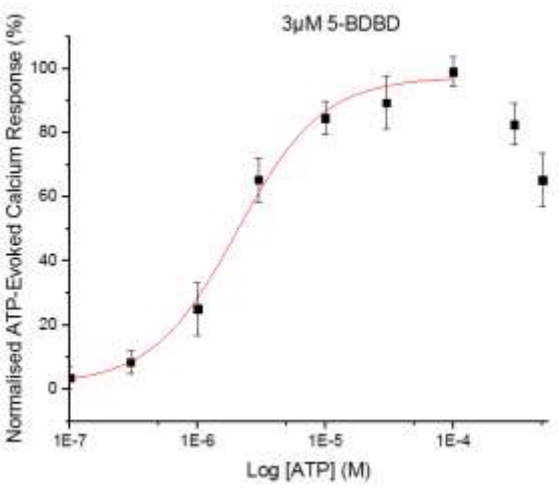

C

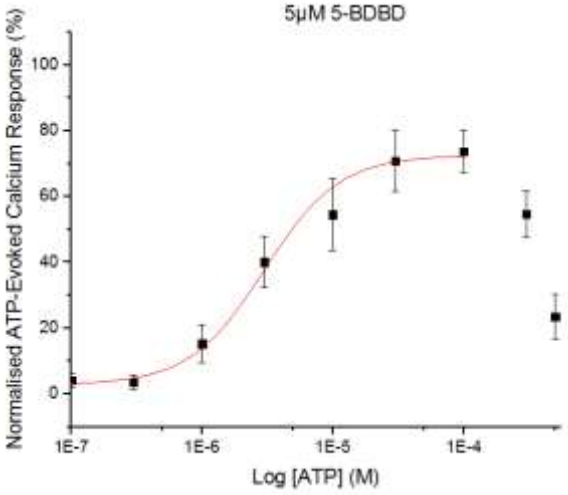

D

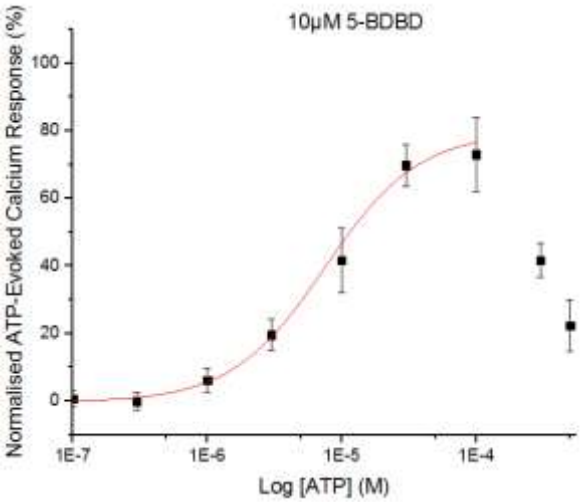

E

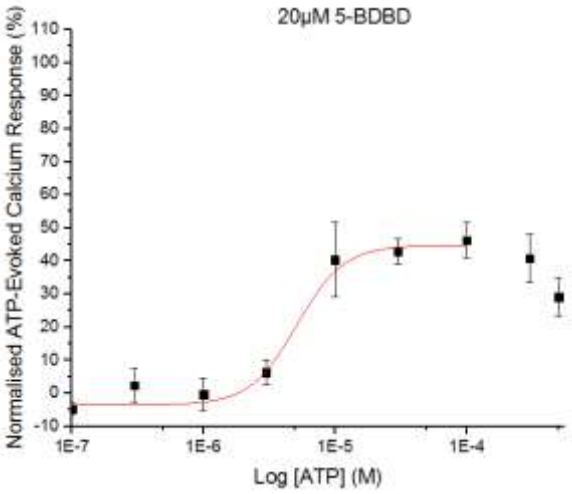

F

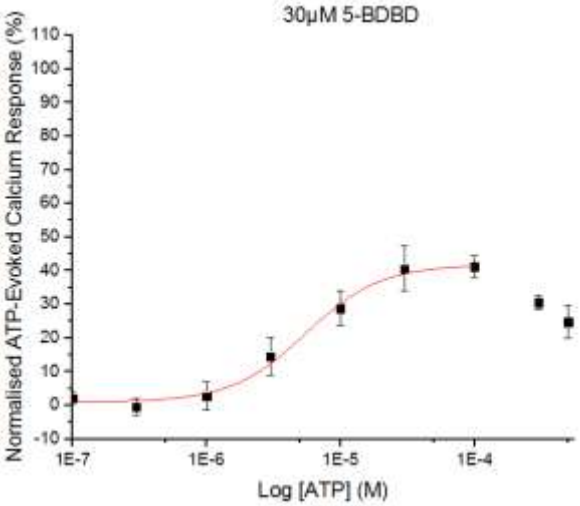

Figure 3.9-ATP does response in the presence for 5-BDBD: Graphs showing an ATP concentration response curve with various concentrations of 5-BDBD. The data was all normalised to an ATP control (30μM) and the graphs were fit with a Hill1 Equation. A) 1μM B) 3μM C) 5μM D) 10μM E) 20μM F) 30μM. Each point has its standard error included (n=5).

In order to see how different 5-BDBD concentrations affect hP2X4, 1321N1 cells expressing this receptor were subjected to 6 different concentrations of 5-BDBD (1μM, 3μM, 5μM, 10μM, 20μM and 30μM). All of the data was normalised to max ATP with no 5-BDBD added to the cells (30μM), which were included on each plate as a control. 1μM gave a higher maximum response than was seen for the ATP control with 104.0 ± 5.8% and 3μM had a very similar maximal response to the ATP control at 99 ± 4.6%. When conducting a Kruskal-Wallis ANOVA, these concentrations were not significantly different from the control. The EC50 values for these two concentrations were 3.1 ± 0.5μM and 3.7 ± 1.4μM as opposed to the 0.4 ± 0.1μM for the ATP concentration response without 5-BDBD. Again however, these were not significantly different from ATP. For 3μM and beyond the concentration of ATP which gives the maximal response has moved from 30μM (which it was for 1μM and the control) to 100μM where it stays for the remainder of the 5-BDBD concentrations. For 5μM of 5-BDBD there was a reduction seen in the maximal response to 75.9 ± 5.2% of the control. The EC50 for this concentration was 2.8 ± 0.6μM however again these were not significantly different from the control values. For 10μM the maximal response given was 70.9 ± 8.4% which was not significantly different. For the EC50 on the other hand, the value of 5.8 ± 1μM was significantly different from the control ($p=0.014$). This tells us that there has been a significant rightward shift of the curve at this concentration. At 20μM there was the first significant reduction in the maxima for the concentrations tested with the maximum response falling to 48.1 ± 4.6% ($p=0.022$). The EC50 value was also significantly different from ATP again at 6.0 ± 1.3μM ($p=0.009$). For the final concentration of 30μM there was again a significant reduction in the maxima and increase in the EC50 value from the control at 41 ±3.1% ($p=0.018$) and 7.2 ± 1μM ($p=6x10^{-4}$) respectively.

Table 2-5-BDBD concentration dependent response: The comparison of different 5-BDBD Concentrations to an ATP Control, with * denoting those which are significantly different from ATP ($p<0.05$).

5-BDBD Concentration (μM)	EC50 Value (μM)	Maximum Response (%)
ATP	0.4 ± 0.1	100%
1	3.1 ± 0.5	104.0 ± 5.8
3	3.7 ± 1.4	99.0 ± 4.4
5	2.8 ± 0.6	75.9 ± 5.2
10	5.8 ± 1.0*	70.9 ± 8.4
20	6.0 ± 1.3*	48.1 ± 4.6*
30	7.2 ± 1.0*	41.0 ± 3.1*

Table 2 shows the amalgamation of the EC50 and maximal response data for the different inhibitor concentrations including the significance from the control and the standard errors at each concentration. There are 3 concentrations which show a significant increase in the EC50 value (10, 20 and 30µM) and two showing a significant reduction in the maximum response (20 and 30µM). As you can see at all 5-BDBD concentrations (although it may not be immediately obvious for 20µM) there was a desensitisation of the receptor at the highest concentrations of ATP meaning that there can be confidence in having achieved the maximal response possible for each of the 5-BDBD concentrations.

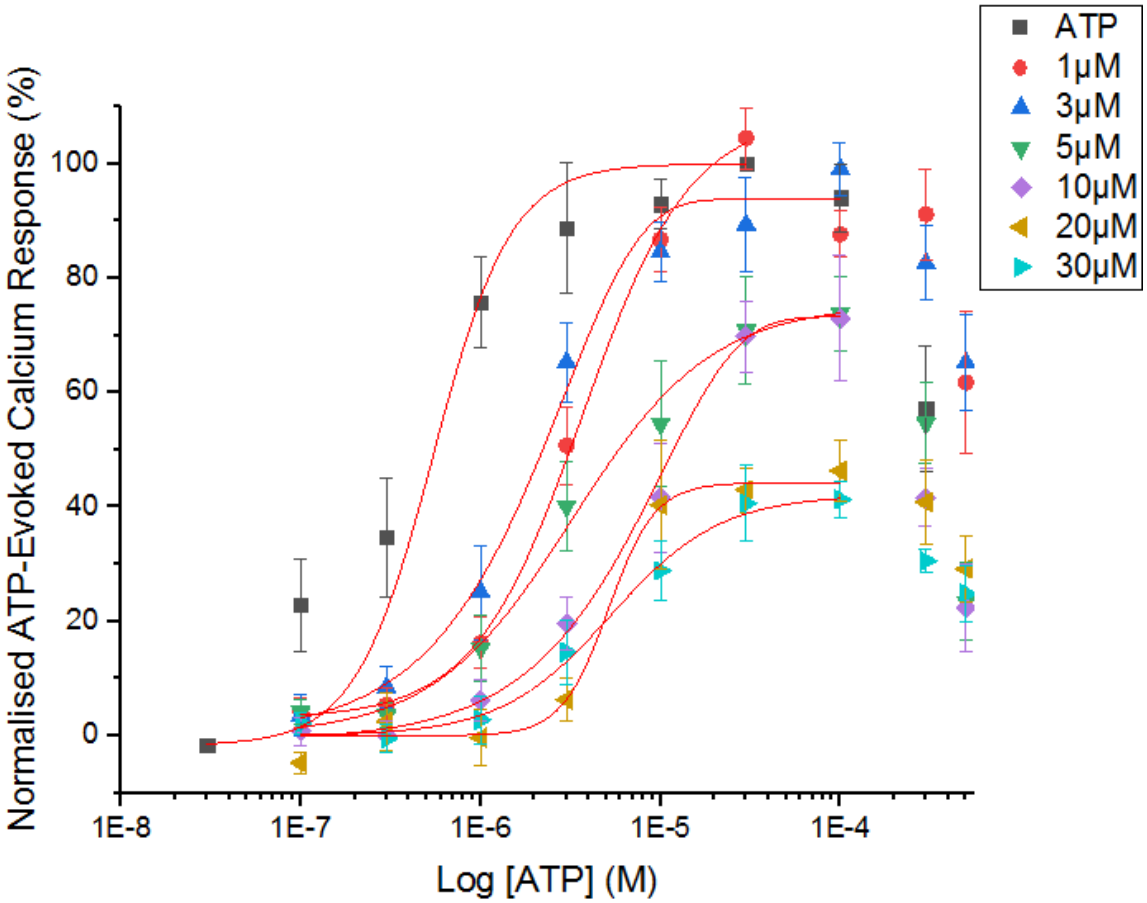

Figure 3.10-5-BDBD ATP concentration response curves on one graph: The amalgamation of data for each of the 5-BDBD concentrations tested and the ATP concentration response which they were compared to. Each of the curves was fitted using the Hill1 equation in order to find the EC50 value for each curve. All the 5-BDBD concentrations were tested against ATP concentrations from 100nM to 500µM. The ATP concentration response curve includes ATP concentrations from 30nM to 300µM (n=5).

Figure 3.10 aligns all the data with curves from each of the 5-BDBD concentrations tested for and the control ATP concentration response curve. This figure helps to visualise the changes in maxima and EC50 value which have been stated as the curves shift to the right when EC50 significantly increases and the height of the curve decreases as the maxima begins to be significantly reduced. As the graph shows, with increasing 5-BDBD

concentration there are two clear trends of right on the X axis and down on the Y axis signifying the decreasing potency of ATP for the receptor and the reduction in efficacy respectively.

3.6 P2X4 Functional Mutant Scan of the Receptor

Due to previous work with P2X4 antagonists which had been conducted in our lab, there was a pre-existing library of chimeric receptors which had 10 amino acid substitutions to the extracellular domain. These stretches of amino acids had been replaced with aligned sequences from P2X2, which section 3.3 showed was relatively insensitive to 5-BDBD.

There were 29 possible mutants that could be made for the receptor encompassing the whole of the extracellular from 55-338 in the primary sequence. Of the mutants tested 21 were functional, meaning that they gave a response to ATP and one mutant was found to have the same sequence of 10 amino acids in both P2X2 and P2X4 when aligned.

These functional mutants were challenged with 30µM of ATP and 20µM of 5-BDBD. There were five wells on each plate with only ATP and 5 wells with ATP and 5-BDBD for each of the mutant receptors. The inhibition in response to 5-BDBD addition was then calculated and presented as a percentage.

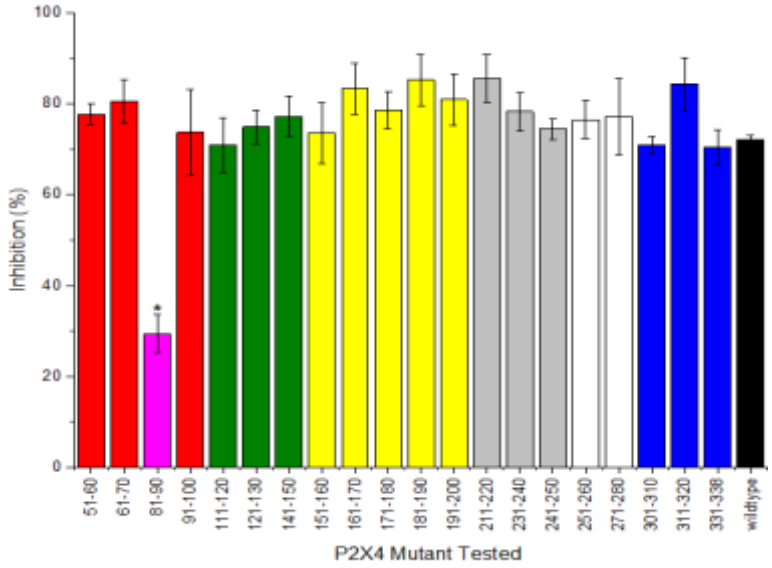

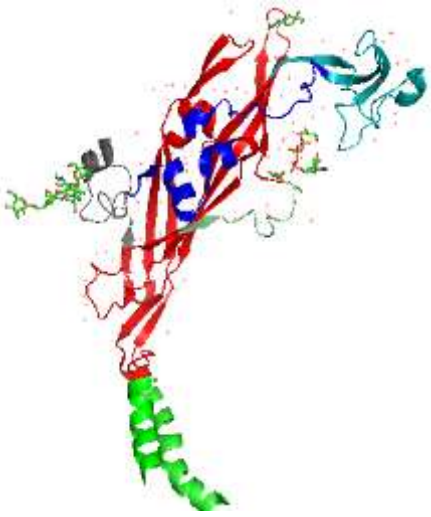

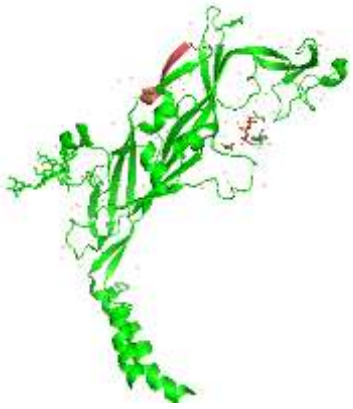

Figure 3.11-P2X4 functional mutant scan, with P2X4 monomer for context: (Left) a scan of functional 10 amino acid mutants for P2X4 showing the percentage inhibition when in the presence of 20μM 5-BDBD compared to only ATP. For all mutant receptors n=5 and for the wildtype receptor n=26. (Right) a figure showing the quaternary structure of a P2X4 monomer with coloured sections corresponding to the colours of the mutants compiling the response reduction graph. Significant difference from the wildtype is denoted with an *. (Bottom) a figure highlighting only the 81-90 region of the P2X4 monomer.

In figure 3.11 above you can see that for almost all mutants there was a consistent level of inhibition with the lowest other than 81-90 being at 70.5 ± 3.8% (331-338) and the highest recorded inhibition being 85.6 ± 5.3% (211-220). 20μM of 5-BDBD caused an average inhibition to the wildtype receptor of 72.1 ± 0.9% which sits well within this range. There was no significant difference between any of these mutants and the wildtype receptor.

For the mutant 81-90 however there was an inhibitionof 29.4 ± 4.3%, showing that this mutant was much less sensitive to 5-BDBD than the others tested in this scan. The 81-90 mutant was significantly different to the wild type receptor ($p=4.8x10^{-4}$) and to all other functional mutants when performing a Kruskal-Wallis ANOVA.

3.7 Point Mutation Within the 81-90 Chimera

Once it had been established that the 81-90 chimera significantly reduced the inhibition of P2X4 by 5-BDBD, point mutations that could be made within this area were considered. Mutation of the 81st residue was chosen as this was the only residue within the stretch which was unique to hP2X4 within the 7 hP2X receptors. This mutation involved replacing a phenylalanine (found at residue 81 of P2X4) with a histidine residue (found at residue 81 of P2X2)

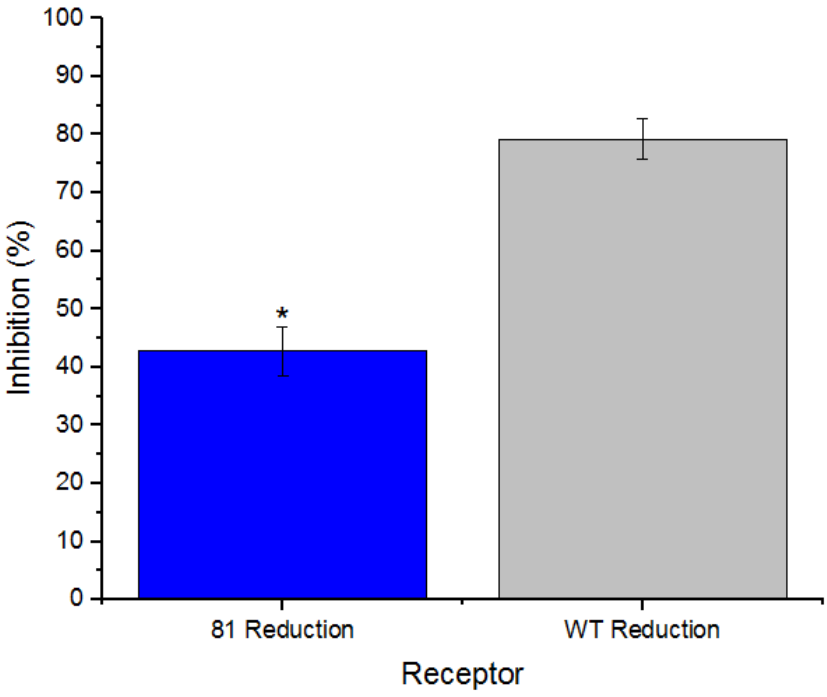

Figure 3.12-A comparison WT to 81-point mutant response reduction: A comparison between the response reductions elicited by 5-BDBD at the wildtype receptor (WT) and the 81-point mutant receptor. There are error bars present and an * to signify a statistically significant difference between the two data sets (p=0.009) (n=5).

When directly comparing the 81-point mutant receptor to the wildtype an ATP concentration of 30µM was used along with 20µM of 5-BDBD. The inhibition at the WT receptor was 79.2 ± 3.5% which was similar to that found in the receptor scan in section 3.6 (72.1 ± 0.9%) with the higher variability due to the lower number of repeats in this experiment. For the 81 mutant the average inhibition was 42.7 ± 4.2%. When performing a Kruskal-Wallis ANOVA the data sets were significantly different (p=0.009) showing that mutation of the 81st residue significantly reduces the inhibitory capability of 5-BDBD.

3.8 ATP Concentration Response Curves for the Mutants of Interest

An ATP concentration response was conducted for both of the mutant receptors of interest in order to see if the mutation made had significantly affected the potency of ATP for the receptor.

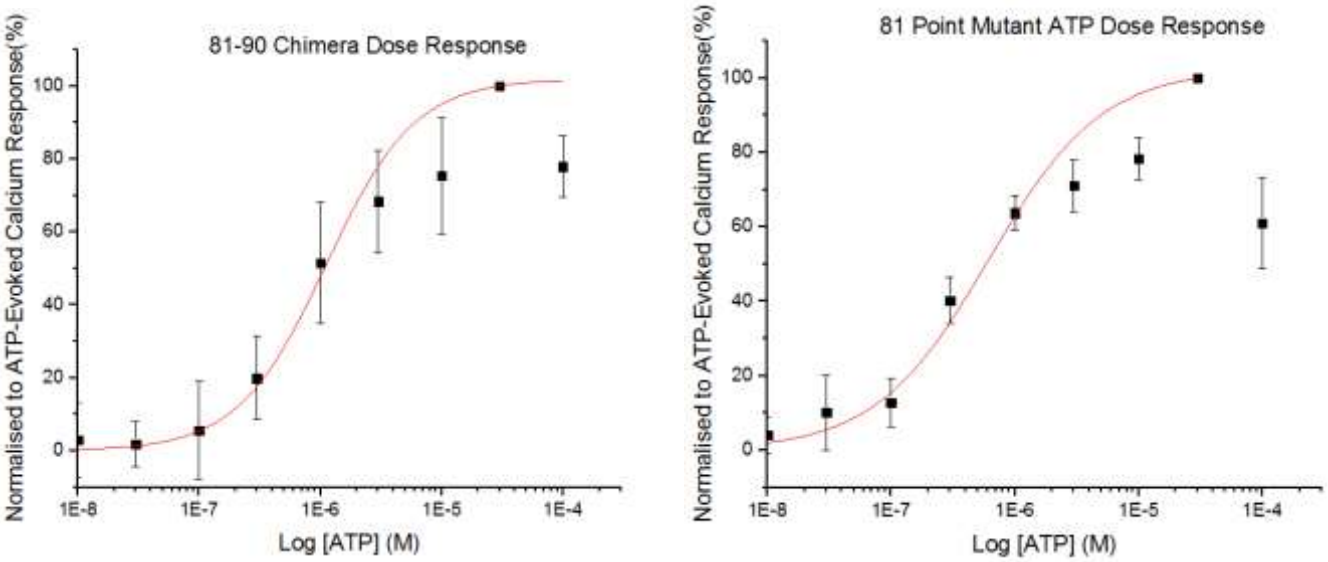

Figure 3.13-ATP concentration response curves for the mutant receptors of interest: Two ATP concentration response curve for the 81-90 chimeric receptor (left) and the 81-point mutant receptor (right). They are both fit with the Hill1 equation in order to aid in the derivation of an EC50. All points are presented with standard error from the five repeats at each concentration for both receptors (n=5).

For both mutant receptors the maximal response was achieved at 30µM and there was a desensitisation at 100µM which was the same as what was seen from the wildtype receptor in figure 3.. The EC50 for the 81-90 chimera was found to be 862.8 ± 318.6nM and for the 81-point mutant it was 573.3 ± 115.3nM. When compared to the EC50 value derived from the wildtype receptor (379.8 ± 99.0nM) using a post-hoc Kruskal-Wallis ANOVA, there was no significant difference between any of the three receptors.

Chapter 4: Discussion

4.1 Transfection Optimisation

1321N1 cells were chosen for this project due to them not endogenously expressing any purinergic receptors (Abbracchio et al, 2016), which would mean that there should be no response to ATP from blank (non-transfected) cells. This would allow for easier analysis of data as the only response given after the addition of ATP should be from hP2X4 in both the stably and transiently transfected cells. This differs from other commonly used cell lines such as HEK293 and HeLa cell lines. HEK cells for instance, endogenously express P2Y receptors which are stimulated by ATP (Schachter et al, 1997; Fischer et al, 2005; Romanov et al, 2007). This means that when looking for P2X4 response in stably transfected HEK cells, the response of blank HEK cells must be subtracted which can lead to variable results and often at high antagonist concentrations give negative results depending on the size of the blank response. In HEK cells expressing P2X4 the majority of the response can often be made up of P2Y receptor activity, providing only a small margin for error when looking at P2X4 activity. In this study the blanks were subtracted from the data gathered, but this was only as a precautionary measure in order to remove the background noise which occurs throughout the assays. Using 1321N1 cells was therefore beneficial as it gave a move clear picture of the effect of 5-BDBD solely on the hP2X4 receptor.

The issue that was found with 1321N1 cells however was that there was little literature denoting the best conditions for transfection of these cells than the lines previously mentioned. Several studies had used 1321N1 cells transfected with GPCR's, however the methods of transfection were often inconsistent or stably transfected cells were used, with this study adopting a transient transfection method (Charlton et al, 1996; Seye et al, 2004; Pugliese et al, 2009). When beginning to plan the optimisation of this protocol there was one paper which was very useful as it tested the effectiveness of several different techniques and some of the more common transfection reagents which were readily available within the lab (Marucci et al, 2011). In this review the group rated the transfection method based on two distinct categories, cell viability and transfection efficiency. Overall, it was found that microporation was the best technique to use for transfection of 1321N1 cells due to it having a ten-fold higher transfection efficiency than any of the other methods whilst having a 75% cell viability (3rd of the 5 methods tested). Microporation having a high rate of transfection efficiency but leading to a slightly lower than optimal cell viability, which is corroborated by several other studies (Lim et al, 2010; Halim et al, 2014), would naturally be seen as the primary method of 1321N1 cell transfection. However, the equipment to perform transfections via this method was not available within the lab.

When looking at the reagent-based transfections described in this transfection optimisation paper (Marucci et al, 2011), FuGene stands out from the others which were also generic transfection reagents, readily available within the lab. FuGene gave the lowest cell viability but the third highest transfection efficiency and when looking at the data collected in section 3.1 this low cell viability may be a reason for the low responses achieved when using this reagent. FuGene in fact gave the lowest responses of the four reagents tested with a maximal F ratio of 0.165, showing that it may be an ineffective reagent for 1321N1 cells

despite being very good at transfecting other cell lines such as HeLa and HepG2 (Yamano et al, 2010). The next reagent tested was Polyfect, there was no documented attempt to transfect 1321N1 cells using Polyfect but again it was a readily available reagent which was adept at the transfection of other cell lines (Breunig et al, 2007). Polyfect didn't produce any conditions which were significantly different from the blank response with a maximal F ratio of 0.21 achieved, meaning that it was not in contention to be used as the reagent in this study.

Thirdly, X-treme Gene is a transfection reagent which has similar properties to another reagent in the paper called Arrest-in (Marucci et al, 2011). Arrest-in was found to have the second highest transfection efficiency and the second highest cell viability, suggesting that X-treme Gene could be one of the front runners. When testing X-treme gene at a range of conditions (similar to the other reagents) it was found that 3 of the 6 conditions gave a response significantly higher than the background with the most efficacious condition being at 0.3µl of reagent and 150ng per well of DNA which gave an F ratio response of 0.24. The Final reagent tested was Lipofectamine. In the aforementioned study Lipofectamine came fourth of five for both cell viability and transfection efficiency. However, Lipofectamine is a common reagent which is often used for RNA transfections and has the benefit of working via lipofection which allows for effective transfection in many cell lines, especially through cell culture methods (Carter et al, 2015). When testing Lipofectamine 4 of the 6 conditions tested gave a significantly higher F ratio than the blank with the highest being at 0.355 (300ng of DNA and 0.5 µl of Lipofectamine per well). This condition gave the best response found across any of the reagents and is the condition set which would be used for the remaining transfections in this project. The reason for Lipofectamine being the most effective transfection reagent in this study may be that it is the only Liposomal reagent of the four tested which may be the preferred method of 1321N1 cell transfection because of the flexibility of lipofection, due to the aversion of this cell line to transfection. This higher range of transfection targets comes from the ability of the liposome containing the DNA to merge with the lipids on the cell surface allowing the contents of the liposome to empty into the cytoplasm of the cell (Balazs et al, 2011). Another possible reason for Lipofectamine being the most effective transfection reagent could be due to the low toxicity of lipofection compared to other methods. Although the 1321N1 cell transfection study (Marucci et al, 2011) ranked Lipofectamine as 4th for cell viability, other studies have shown that Lipofection causes low toxicity to the cells which could explain the higher responses found when using this reagent (Maurisse et al, 2010, Wang et al, 2018).

4.2 hP2X4 and hP2X2 EC50 and IC50 Value Derivation

When looking at the ATP concentration response data generated in this study, an EC50 of 479nM was derived for P2X4 which was significantly different from the P2X2 value of 1µM. This EC50 for P2X2 is similar to that found in several studies (North et al, 2009; Li et al, 2013; Ding et al, 1999). The significant difference between the two receptors suggests that there is a difference in the potency of ATP for the two. P2X2 being further to the right on an ATP concentration response would suggest that ATP is a less potent agonist for hP2X2 than it is for hP2X4. The other key difference that can be seen between the two receptors is that there is a desensitisation of the channel for P2X4 at 100µM and 300µM which does not occur for P2X2. This desensitisation is common for hP2X4 (Sim et al, 2007) and can be due to receptor internalisation at the cell surface or over-competition at the ligand binding site. The lack of desensitisation for P2X2 could be due to this receptor having a much slower rate of desensitisation which may not be seen within the 250 seconds of each assay (Volonte et al, 2009). An approximate EC50 ATP concentration (500nM for P2X4 and 1µM for P2X2) was used in the derivation of an IC50 value for each of the receptors moving forward.

An IC50 of 873.9nM for 5-BDBD was derived from P2X4 with the maximal inhibition of response being 95% of the control. This IC50 was slightly higher than the 500nM found in 2005 (Fischer et al, 2005) and slightly lower than the 1.2 µM found by Balasz's group (Balasz et al, 2013) although this was conducted using patch clamp electrophysiology rather than a Flexstation III which can lead to higher IC50 and EC50 values. The derivation of an IC50 value allows for the comparison of the potency for different inhibitors of the same receptor. At P2X4 for example we can compare the potency of 5-BDBD to other selective P2X4 antagonists such as BX430 and PSB12054. For BX430 an IC50 value of 540nM was found when using patch clamp analysis (Ase et al, 2015) and 1.6µM when performing a Ca^{2+} assay with a Flesxstation III (Layhadi et al, 2018). PSB-12054 on the other hand using patch clamp an IC50 of 190nM was derived (Ase et al, 2015) and using a Ca^{2+} influx assay it was found to be 189nM (Hernandez-Olmos, 2012). These three selective antagonists can therefore be compared for potency using the calcium-based assays for reference due to the nature of this study. 5-BDBD based on the evidence is a more potent inhibitor than BX430 and less potent that PSB-12054 giving a ranking of PSB-12054>5-BDBD>BX430.

An IC50 value could not be derived for P2X2 due to not being able to fit a Hill1 equation to the data. This occurred due to the lack of inhibition seen for the concentrations tested. There was no concentration -dependent inhibition of the receptor seen, with there was no significant difference between any of the concentrations in this range. The 5-BDBD concentrations 10nM to 10µM all had responses of between 85% and 102% of the control response, indicating that 5-BDBD has little or no effect on P2X2 Ca^{2+} response within this range. Moving forward the 5-BDBD concentration used for screening mutants was agreed to be 20µM as this caused an 85% reduction in P2X4 response without significantly reducing P2X2 response (14% reduction).

The range of concentrations used for IC50 value derivation (300pM to 50µM) was larger than for EC50 (10nM to 300µM). For IC50 curves two different concentration ranges were used, 300pM to 50µM for P2X4 and 10nM to 30µM for P2X2. The reason for the P2X4 IC50

concentration range going to such a low point was due to issues found when trying to use 10nM or 30nM as the lowest concentrations in preliminary tests. The issue with using these concentrations as the lowest in the study was that 5-BDBD has not titrated back to 100% of control response, meaning that 5-BDBD was still having a small inhibitory effect on the receptor at this concentration. This was not the case for P2X2 as at 10nM the Ca^{2+} response was already at 100% of control response so no smaller concentrations were required to be tested. It can be seen in figure 3.6 that at 30nM the normalised response is still below 100% of the control and that the data had not plateaued at this point meaning that it is difficult to fit a Hill1 equation to the curve, making the derivation of an IC50 value more difficult. For these reasons the range of 5-BDBD concentrations tested against hP2X4 was extended at the lower end to 300pM.

The trace data in section 3.4 is a clear indication of the effect 5-BDBD has on a normal P2X4 response. The Flexstation trace is key to all of the results collected in this study as the peak response from each trace, for each well tested is the primary data point which allowed for the comparison of different conditions in this study. In figure 3.8 it can be seen that 5-BDBD reduces the peak F ratio by 47.4% which is similar to the response reduction found when running under the same conditions in section 3.5 (52.0% response reduction). Figure 3.8 also shows that the shape of the graph changes with there being less of a rapid increase to the peak F ratio after the addition of agonist (usually occurs within 10 seconds of addition). For the trace with 5-BDBD present the peak is reached after 110 seconds of the assay. This changes another metric which the inhibition of 5-BDBD could be measured by: area under the curve. In this study peak F ratio was used rather than area under the curve due to the ease of data analysis when conducting the receptor scan and the fact that the 'peak' response achieved is not dependent on both the rate of desensitisation and the maximal response achieved in the assay. This should mean that using the peak response metric rather than area under the curve should lead to a lower variability across the data set. However, if this project was to be repeated using both of these metrics throughout could be interesting to see how 5-BDBD effects the amplitude of response and the trace data.

4.3 5-BDBD concentration Response

In this study, the lower concentrations of 5-BDBD tested for (up until 10µM) showed no significance in either EC50 value or maxima reduction from the control. One influential study showing the action of 5-BDBD concluded that there was a rightward shift in the ATP concentration response curve, without the maximal response changing and therefore that 5-BDBD is a competitive antagonist (Balasz et al 2013). This is due in some part to the small number of concentrations which were tested for in the study conducted by this group, who noted the difference between ATP (control), 2µM and 20µM. There only being two concentrations of 5-BDBD and the wide difference between these two may prevent the small changes in maxima and EC50 being picked up. In this project 3µM and 20µM are almost equivalent to the 2µM and 20µM used in the aforementioned study. In section 3.5 it can be seen that 20µM had a significantly higher EC50 than the control but 3µM did not. If only looking at this metric you can assume that the increase in EC50 and shift rightwards on the concentration response curve shows that 5-BDBD is competitive. However, at 20µM

there is also a significant reduction in the maxima from the control shown in figure 3.9 and table 2. In the study conducted by Balasz's group there was 'no change in the magnitude of maximal stimulation'. This difference found between the two studies may be due to the different methods used, with patch clamp being employed for Balasz's study and this study using a Flexstation based protocol. Based on the different cations being tested for in these protocols (sodium for patch clamp and calcium for the Flexstation) and the contrast in data collection methods, this could explain the differences in the maximum response elicited after 5-BDBD addition.

The data in table 2 shows that with increasing 5-BDBD concentration there are two clear trends. An increase in EC50 value and a decrease in normalised maximal response achieved. In terms of EC50, this trend becomes statistically significant for 10µM and above. For the maximal response, it is significant at 20µM and 30µM only. This could be a reason for the belief that 5-BDBD is non-competitive, as tests using lower concentrations with small incremental changes may see the change in EC50 value before the reduction in maxima. This can be seen with the differences between ATP, 1µM and 3µM in my study. The maximal response achieved at these concentrations were 100%, 104% and 99% respectively which when plotted on a concentration response curve will show almost no difference in the maximal response but the EC50 value changes from 0.38 µM (ATP) to 3.1 µM (1µM) and 3.7 µM (3µM), which will be more easily visible due to the rightward shift of the curve.

This may be the reason that testing the action of 5-BDBD at low concentrations can produce the thought that it acts competitively as there is a trend to the right between these two concentrations, but the max response remains very similar. This shift, without a reduction, was also documented by a previous member of my lab (Bin Ahmad, 2018) who found that addition of 1.9µM of 5-BDBD (the derived IC50) caused a rightward shift of the concentration response curve and gave a significantly higher EC50 value than ATP without 5-BDBD, without affecting the maximal response. Based on this data it would be appropriate to conclude that 5-BDBD acts competitively. However, based on 20µM and 30µM significantly reducing the maxima, it would be more appropriate to say that it shows mixed modality in this study. The working explanation for this may be that the antagonist binds to an allosteric site which is close to the agonist binding site. This can affect agonist binding at low concentrations resulting in the mode of action looking competitive at low concentrations but eliciting a non-competitive effect at higher concentrations. A second theory for why this occurs could be due to there being two or more sites where 5-BDBD can bind to the receptor. The higher affinity site could be in or near the agonist binding site and a lower affinity site, at an allosteric location. From the data collected it can be taken that 5-BDBD acts non-competitively at human P2X4. Thirdly, the explanation could be that 5-BDBD binding to an allosteric site on P2X4 could cause these effects in tandem as there are other allosteric inhibitors which can have mixed modal effects on their targets.

4.4 Functional Mutant Receptor Scan

When conducting a scan of the receptor to look for areas of interest, a similar method had previously been used in a similar study (Ase et al, 2019) where several residues were mutated using a PCR based mutagenesis method in order to find residues which were key to BX430 action at P2X4. How this experiment differed however is that instead of mutating single residues which had been found to be conserved between the different species which were sensitive to BX430, 10 amino acid stretches of the receptor's extracellular domain were replaced with aligned sections from P2X2 which was shown to be significantly less sensitive to 5-BDBD than P2X4 for the concentrations tested.

When conducting the scan in section3.6, 5 repeats without 5-BDBD and 5 with 5-BDBD were compared to see the inhibition caused by 20μM of the inhibitor. If there is a section of the receptor which may be important for 5-BDBD action, you would expect to see a significantly lower inhibition due to potentially important residues within that mutant being removed.

In the scan of the receptor, it appeared that all bar one of the mutants were within a tight range between 70.5% and 85.6%, comparable to 5-BDBD inhibition of the wildtype receptor. This would suggest that the stretch of amino acids which had been replaced were not necessary for 5-BDBD action because if a residue which is essential to 5-BDBD action is removed you would expect to see a significant reduction in percentage inhibition. For one mutant however (81-90), there was a significant reduction in inhibition when challenged with 5-BDBD. Indicating that this region does contains one or several residues which may be important in eliciting the action of 5-BDBD at hP2X4.

This region may be important as it is just upstream of two key residues, K70 and K72, which are involved in ATP binding as they control the coordination of oxygens on the phosphate groups (K70) and the coordination of γ-phosphate groups (K72). 81-90 is the closest functional mutant to the binding site on this side of the monomer as the 71-80 mutant was non-functional, possibly due to removal of these important residues. This would likely result in the 71-80 mutant not being able to coordinate the ATP molecules in the binding groove, resulting in no response to ATP (what was deemed as a non-functional). K70 and K72 are found in the binding pocket between the left flipper and head domain, towards the head at the edge of this pocket. 5-BDBD interacting with the receptor within close proximity to the ligand binding site could explain the mixed modal effects that are seen in the 5-BDBD ATP concentration response section (3.5). If the molecule interacts with the receptor closely to the ligand binding site it could perturb the entry of ATP at lower concentrations as it may obscure part of the entrance, leading to the decrease in potency of ATP for the receptor seen. At higher concentrations of 5-BDBD this effect on potency could still be present in the form of reduced ATP entry but then be outweighed by the allosteric effect of the inhibitor. This allosteric effect causes the decrease in efficacy seen in section 3.5. The allosteric effect elicited by 5-BDBD is likely to be due to a change in the conformation of the channel or the receptor dynamics (Nusinov and Tsai, 2013). Traditionally it was thought that binding of an allosteric inhibitor leads to a conformational change of the protein (Tsai et al, 2009) but formal descriptions of allosteric now include changes in dynamics for the protein (Hilser et al, 2012). This means that the interaction of 5-BDBD with this allosteric site could cause a

change in shape of the ligand binding site, resulting in a reduction in efficacy or a change in channel dynamics such as perturbing the flexing of the lower body domain of P2X4, therefore impeding the activity of P2X4.

4.5 Residues Phenylalanine 81 to Valine90

When there had been statistical confirmation that the 81-90 chimera was an area of interest for this study, a more in-depth analysis of this region was undertaken including a direct sequence comparison between hP2X4 and the other human P2X receptors.

Table 3-An alignment of the 7 P2X receptors in humans between residue 81 and 90: An aligned comparison between the 7 P2X receptors in humans, with a particular focus on the residues from 81 to 90 in the primary sequence. The highlighted residues were possible mutation points.

	Aligned P2X									
P2X Receptor	81	82	83	84	85	86	87	88	89	90
P2X1	P	Q	V	W	D	V	A	D	Y	V
P2X2	H	K	V	W	D	V	E	E	Y	V
P2X3	N	R	V	M	D	V	S	D	Y	V
P2X4	F	R	I	W	D	V	A	D	Y	V
P2X5	Q	R	I	W	D	V	A	D	Y	V
P2X6	N	R	L	W	D	V	A	D	Y	V
P2X7	H	S	V	F	D	T	A	D	Y	T

Using table 3 we were able to visualise the differences in residues between the P2X receptors in humans, these differences could be key to 5-BDBD inhibition due to it being selective for P2X4 over other receptors in the family (Jacobson and Muller, 2016). If the selectivity that 5-BDBD has for P2X4 is due to an interaction which occurs with the receptor at one or multiple residues within this area, it would stand to reason that the residue would be unique to P2X4 or at least possessed by few other P2X receptors.

When comparing the Sequences three areas within this group stood out, two for being fairly unique and one for being different to P2X2 which was used in the study when making chimeras and point mutations. These key residues were highlighted in table 3 above as green (81st residue), yellow (83rd residue) and blue (the 87th and 88th residues). All other residues were conserved between P2X2 and P2X4 other than residue 82 where P2X2 has a Lysine instead of an arginine. This difference should does not stand out however as the amino acids are both positively charged and are of a similar size with arginine being the larger of the two. Arginine is also shared by 3 of the other P2X receptors rendering it unlikely to be a residue of interest.

4.5.1 Residue Phenylalanine 81

The 81st residue (a phenylalanine) was marked as of interest as it is shared by none of the other P2X receptors and this residue is one which is the most variable within the stretch with 5 different amino acids between the receptors (the most of any residue in this alignment) and being the only residue which doesn't have a single amino acid shared by four or more of the P2X receptors (82nd and 83rd both having four which share arginine and valine respectively). When looking at differences between the chosen residues it is most important to understand the difference between the P2X4 and P2X2 amino acids as P2X2 has been used in the mutant scan and will be used to make any point mutant. For the 81st residue in P2X4 there is a phenylalanine which is a non-polar amino acid with an aromatic r-group. For P2X2 at this residue a histidine is present (also found for P2X7) which is positively charged and has an imidazole functional group. This difference in polarity between the two residues could account for the interaction of 5-BDBD selectively over P2X2. When looking at the amino acids which the other P2X receptors possess at this point; asparagine (P2X3 and P2X6) and glutamate (P2X5) are both polar uncharged amino acids. The only receptor which has non-polar amino acid at residue 81 is P2X1 which has a proline.

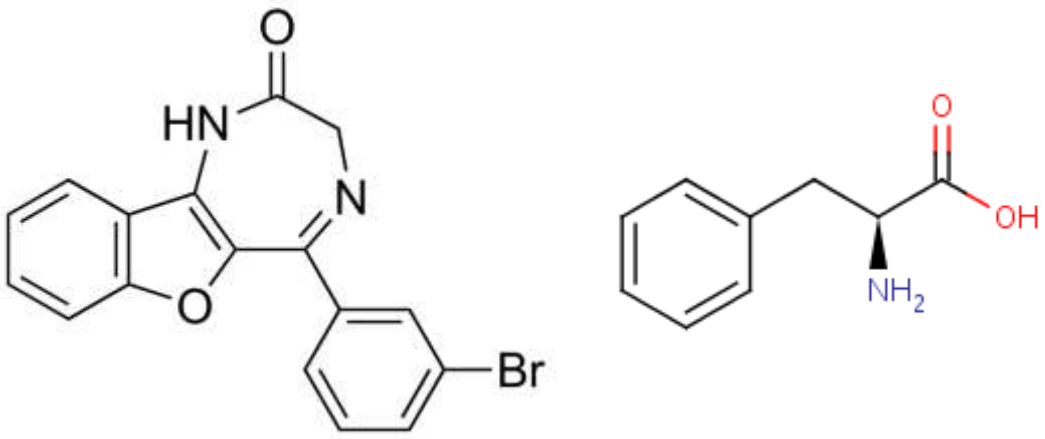

Figure 4.1-The chemical structures of 5-BDBD and Phenylalanine: The chemical structures of 5-BDBD (left) and Phenylalanine (right) showing their functional groups. There being two aromatic rings on 5-BDBD one on the middle left and one on the bottom right of the molecule, for Phenylalanine the ring can be seen on the left of the molecule (Sigma Aldrich, 2019; ChEBI, 2019).

There are two clear distinctions between phenylalanine at P2X4 and the other amino acids present in the other 6 receptors. Firstly, is that all bar P2X1 has a polar residue, where P2X4 has a non-polar residue. This would however rule out 5-BDBD being attracted to P2X4 due to its polarity as non-polar molecules will not attract each other based on their polarity. Secondly that phenylalanine is the only amino acid which has an aromatic r-group. When looking at the structure of 5-BDBD it has two aromatic groups one with a bromide attached and one attached to the main bulk of the molecule. With phenylalanine having an aromatic group it would stand to reason that one of the aromatic groups from 5-BDBD and the aromatic group from phenylalanine at residue 81 in P2X4 could interact via a process called stacking. This interaction occurs due to the alignment of opposing electrostatic potentials between the electrons in the pi rings of the two aromatic groups (Wheeler et al, 2014). The

small positive charge from one ring attracts the small negative charge from the other, producing a non-covalent interaction between the two rings (Rahman et al, 2015). The fact that P2X4 is the only receptor in the family which has an amino acid with an aromatic group at this point would suggest that this is more likely to be the reason for 5-BDBD interacting at point 81 than the polarity of the amino acids at this point in the other receptors, especially bearing in mind that P2X1 also has a non-polar amino acid at this point.

4.5.2 Residue Isoleucine 83

The second residue of interest in this section is at position 83. For P2X4 at this point the amino acid is isoleucine which is only shared by one other receptor in the family P2X5. When looking at which amino acids are present for the receptors there is valine (P2X1, 2, 3 and P2X7) and leucine (P2X6). When looking at the properties of these amino acids they are all non-polar and all have aliphatic r groups. This shows that the amino acids will only be marginally different chemically, resulting in there being little room for selectivity based on this residue alone.

4.5.3 Residue Alanine 87 and Aspartic Acid 88

For residue 87 and 88 there were many receptors in the family which shared the same amino acids at this point (alanine and aspartic acid respectively) with P2X1,P2X4,P2X5, P2X6 and P2X7 all having A and D at residue 87 and 88. When comparing these residues to P2X2 however there was a difference which was studied to see if this region could be important. At P2X2 residue 87 and 88 are both glutamic acids. For position 88 for both receptors the amino acids are polar with acidic r groups, with the only difference being the length of the r group chain. At position 87 on the other hand, an alanine which is non polar with an aliphatic r group is substituted for a polar and acidic glutamic acid. This would result in a more highly charged section of the receptor which may repel the 5-BDBD and stop it from binding to hP2X2. However, whilst this would account for the selectivity of 5-BDBD for hP2X4 over P2X2, it would not account for its selectivity over the other P2X receptors with 4 sharing these two residues.

When looking at this region of the receptor for humans, rats and mice it can be seen that from 81-90 is conserved between the species providing possible evidence for why 5-BDBD is able to antagonise rat and mouse P2X4 (Coddou et al, 2018: Yu et al, 2018: Ledderose et al, 2018). Adding further weight to the conclusion that one of the residues within this region plays a role in 5-BDBD action.

Overall based on the evidence presented it was clear that P2X4 selectivity for 5-BDBD comes from within the 81-90 region and that the most likely point of interaction for the inhibitor would be at residue 81. This is not only due to it being unique amongst the other receptors in the primary sequence, but also the presence of an aromatic group providing a method of interaction with 5-BDBD.

4.5.4 Residue 81 Percentage Inhibition Derivation

Once residue 81 had been singled out the point mutant was produced and tested for the inhibition elicited by 20μM of 5-BDBD, in much the same way as for the scan of the receptor in section 3.6.

The WT inhibition was 79.2 ± 3.5% which is higher than was found for the overall scan of the receptor, but this would be due to the number of repeats which were undertaken for the WT receptor in this section resulting in less standard error and a truer value for than in section 3.7. The inhibition found was however well within the normal range specified of 70.45% to 85.59%. For the point mutant the inhibition was 42.7 ± 4.2% which is significantly lower than at the wildtype ($p=0.009$) suggesting that this mutation significantly reduced the sensitivity of the receptor to 5-BDBD.

When comparing the 81-point mutant to the 81-90 chimera which stood out from section 3.6, the point mutant has a higher inhibition (13.3%) than the chimera suggesting that it conveys less sensitivity to 5-BDBD. However, when performing a Kruskal-Wallis ANOVA there was no significant difference between the two data sets ($p=0.076$). This difference in sensitivity for 5-BDBD may suggest that 5-BDBD interacts with more than one residue in this stretch of the receptor. This would however presumably lead to issues with selectivity for P2X4 over the other receptors unless the 81st residue was a higher affinity interaction site and a further residue or section within the 81-90 region accounts for a lower affinity interaction site. This would account for the reason that at high concentrations of 5-BDBD P2X1 and P2X3 are slightly inhibited in rats (Coddou et al, 2019). However, when looking at the possible areas of interest within the 81-90 region, neither residue 83 or 87 and 88 show a connection to P2X1 or P2X3 over the other receptors in the family. Leading to the possible conclusion that with a higher n number for both the chimera and point mutant, they become more similar in inhibition.

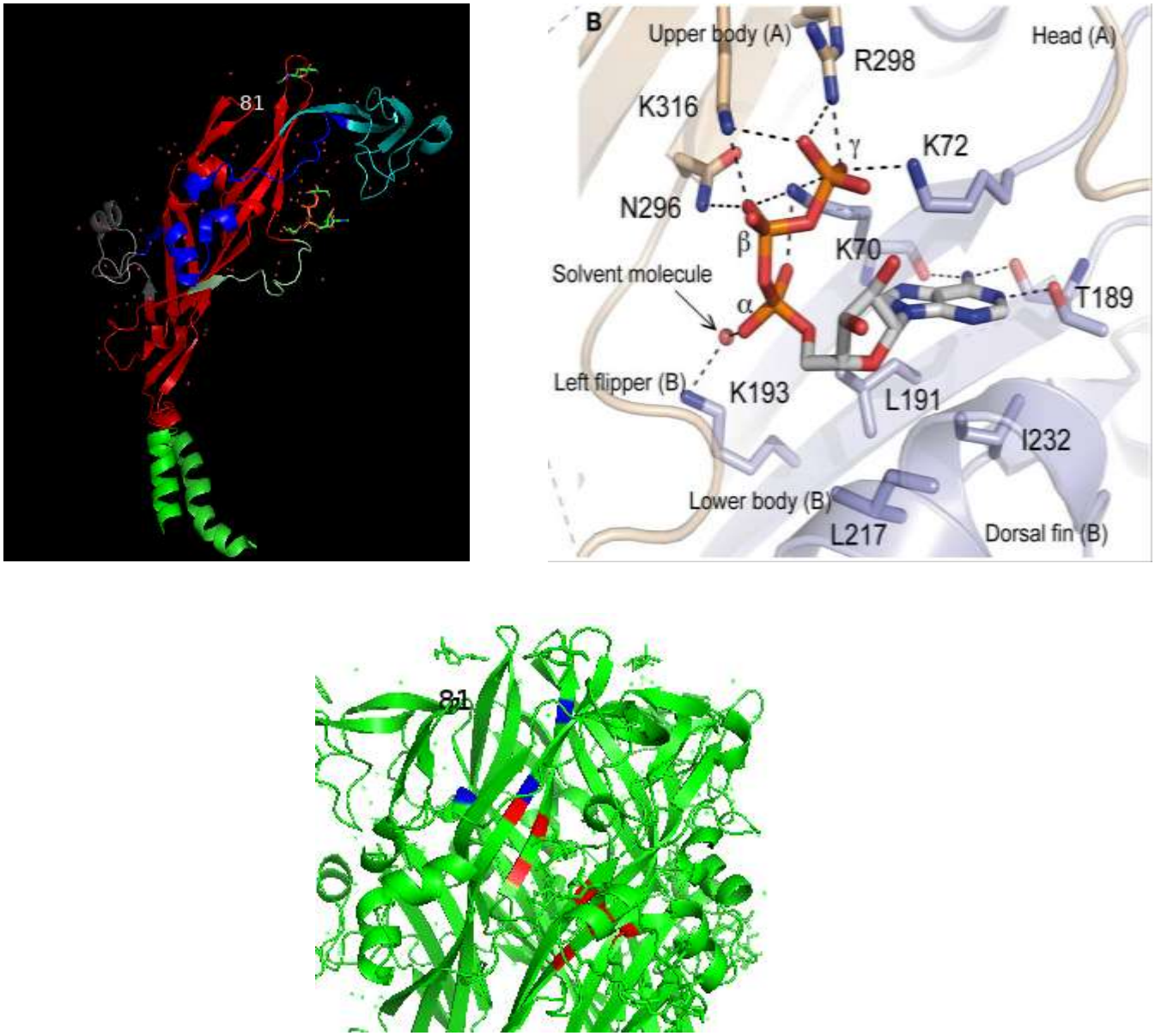

Figure 4.2-The P2X4 ATP binding site relative to residue 81: (Left) A colour coordinated image of a P2X4 monomer with the transmembrane (green), body (red), dorsal fin (dark grey), head (turquoise) right flipper (light grey) and left flipper (blue) domains marked in their own colours to give context for the position of residue 81 in regard to the other features of the monomer. (Right) A diagram showing the points of interaction between an ATP molecule and the two subunits in a functional trimer of the receptor with A denoting the contribution from one monomer and B the contribution from another. Figure taken from a paper published by Chataigneau (2013). (Bottom) An image showing the position of the 81st residue on the P2X4 trimer in relation to the ATP binding site (key residues coloured red) and the binding site for BX-430 found in the Ase paper (Ase et al, 2019) (key residues coloured in blue).

Figure 4.2 shows the colour coordinated P2X4 monomer with the distinct domains highlighted in a different colour and with 81 denoting where the residue of interest is situated. On the right of this figure the interactions between the neighbouring monomers and ATP can be seen with the residues from subunit B coming from the tip of the dorsal fin, the left flipper domain and the lower body domain. This would mean that the ATP binding site is indeed just downstream of the residue of interest (81) which could suggest that the interaction of 5-BDBD with the receptor at residue 81 could perturb ATP entry into the

binding pocket at low concentrations as had been hypothesised. When looking at the bottom image of figure 4.2, the position of residue 81 is relatively close to the ATP binding site and very close to the binding site for BX-430 (another small molecule allosteric inhibitor of P2X4) which was identified in a 2019 paper (Ase et al, 2019). In the aforementioned paper, the group mutated single residues within a region of the ectodomain which was highly conserved among the receptor family. They found that when residue Ile315 (in zebrafish, Ile312 in humans) was mutated to a threonine residue, there was a large reduction in sensitivity of P2X4 for BX-430. In this paper they also found that sensitivity to BX-430 can be restored in rats and mice (which are insensitive to the inhibitor) via inserting isoleucine at this position. The suggested mechanism of action for BX-430 in this paper is through a structural locking of the ectodomain in this specific region caused by the binding of BX-430 at the site. Due to the exceedingly close proximity of residue 81 to this BX-430 this could be a possible mechanism of action for 5-BDBD also, causing a locking of the receptor in a closed state and therefore not allowing the entry of calcium ions into the cell.

There are examples of allosteric inhibitors which can both reduce maximal response and reduce potency of an agonist without being close to the ligand binding site. This is the case for papaverine which is a non-selective smooth muscle relaxant which is most often used as a drug to induce vasodilation (Sonnenfield et al, 1980; Tanyeli et al, 2019). When looking at a concentration response curve for this receptor antagonist there are similarities to what is seen for 5-BDBD with a reduction in the maximal response and a reduction in potency with higher concentrations (Ameer et al, 2010). As papaverine is a non-selective antagonist and elicits its effect through several receptors it is likely that the mixed modality of this inhibition is due to the activity of the antagonist rather than its positioning in regard to the ligand binding site.

4.5.5 Mutant Receptor ATP Concentration Response Curves

In figure 3.14 the two receptors of interest were challenged with the same range of ATP concentrations as the wildtype receptor for the derivation of its EC50. This was done in order to derive an EC50 for the two mutant receptors and see if there was any significant difference in potency of ATP for the mutant receptors over the wildtype. Any changes in ATP potency for these receptors could be a cause for the lower response reductions seen when testing these receptors with 5-BDBD.

When comparing the average EC50 values for the receptors a p value of 1 was found when comparing the 81-point mutant to both the wildtype receptor and the 81-90 chimera. When comparing the 81-90 receptor to the wildtype $p=0.45$. As the level for significance is $p<0.05$ it can be seen that the differences between the receptors in terms of ATP potency are not close to the level of significance. This allows me to be sure that the effect seen with both of these mutant receptors (the lower response reduction) was due to one of the residues which were changed eliciting the effects of 5-BDBD on P2X4 rather than the substitution affecting ATP potency and therefore causing the effects seen.

4.6 Conclusions

Based on the results found in this project, several conclusions can be made regarding the antagonism of hP2X4R by 5-BDBD. Firstly, I would conclude that, in contrast to the consensus view in the published literature, 5-BDBD is a non-competitive antagonist due to the results obtained in section 3.5 which show that unlike a competitive antagonist, 5-BDBD causes a reduction in efficacy and a decrease in potency of ATP for the receptor. This effect would be atypical for a purely competitive antagonist and so led to the pursuit of an allosteric binding site for 5-BDBD. The second conclusion to take is that 5-BDBD interacts with residue 81 in the primary sequence which is situated on the lower body domain of the P2X4 monomer, just upstream from the ligand binding site. This residue is unique to P2X4 within the receptor family and is likely to confer the selectivity of 5-BDBD for P2X4 over the other 6 receptors. This selectivity is likely to come due to the aromatic groups of 5-BDBD and the phenylalanine residue at position 81 'stacking' which allows 5-BDBD to uniquely interact with this receptor. The final conclusion to take is that residue 81 is important for facilitating the inhibitory effects of 5-BDBD on hP2X4 receptors as replacement of this residue with a histidine (present at residue 81 in P2X2) leads to a significant reduction in sensitivity to 5-BDBD. This would suggest that residue 81 can confer sensitivity of the receptor to 5-BDBD.

With this increased understanding of one of the few selective antagonists for P2X4, the hope is that antagonism of this receptor can be better understood and the movement towards a therapy for the pathophysiological processes which it underpins can be increased as more information about this receptor is elucidated. Further studies using this antagonist could aim to find any other potential allosteric site within the non-functional mutant regions of the receptor. Future studies may also endeavour to find the mechanistic properties of 5-BDBD which could aid in the production of further small molecule antagonists for P2X4. Furthermore, computer modelling of 5-BDBD binding to hP2X4 could allow for a certainty around whether 5-BDBD has a single of multiple allosteric sites on the receptor.

References

Abbracchio MP, Ceruti S. P1 Receptors and Cytokine Secretion. *Purinergic Signalling*. 2007; 3(1-2):13–25.

Abbracchio MP, Verderio C. Pathophysiological roles of P2 receptors in glial cells. *Novartis Foundation Symposium*. 2006; 276:91-103.

Abdelrahman A, Namasivayam V, Hinz S, Schiedel AC, Köse M, Burton M, El-Tayeb A, Gillard M, Bajorath J, Ryck M, Müller CE. Characterization of P2X4 receptor agonists and antagonists by calcium influx and radioligand binding studies*. Biochemical Physiology*. 2017; 125:41-54.

Ameer OZ, Salman IM, Najim HS, Abdullah GZ, Abdulkarim MF, Yam MF, Sadikun A, Asmawi MZ. *In Vitro* Pharmacodynamic Profile of *Loranthus ferrugineus:* Evidence for Noncompetitive Antagonism of Norepinephrine-induced Vascular Contraction. *Journal of Acupuncture and Meridian Studies*. 2010; 3(4):272-282.

Ase AR, Honson NS, Zaghdane H, Pfeifer TA, Séguéla P. Identification and characterization of a selective allosteric antagonist of human P2X4 receptor channels. *Molecular Pharmacology***.** 2015; 87(4):606-616.

Ase A, Therrien E, Seguela P. An Allosteric Inhibitory Site Conserved in the Ectodomain of P2X Receptor Channels*. Fronteirs in Cellular Neuroscience*. 2019; 13:121.

Balázs B, Dankó T, Kovács G, Köles L, Hediger MA, Zsembery A. Investigation of the inhibitory effects of the benzodiazepine derivative, 5-BDBD on P2X4 purinergic receptors by two complementary methods. *Cell physiology and Biochemistry*. 2013; 32(1):11-24.

Balazs DA, Godbey WT. Liposome for use in drug delivery. *Journal of Drug Discovery*. 2011; 326497:1-12.

Banfi C., Ferrario S., De Vincenti O., Ceruti S., Fumagalli M., Mazzola A. P2 receptors in human heart: upregulation of P2X6 in patients undergoing heart transplantation, interaction with TNFalpha and potential role in myocardial cell death. *Journal of Molecular and Cellular Cardiology*. 2005; 39:929–939.

Berridge Mj. Calcium signalling remodelling and disease. *Biochemical Society Transactions*. 2012; 40(2):297-309.

Bo X, Kim M, Nori SL, Schoepfer R, Burnstock G, North RA. *Cell Tissue Research*. 2003; 313(2):159-165.

Bootman MD, Collins TJ, Peppiatt CM, Prothero LM, MacKenzie L, De Smet P, Travers M, Tovey SC, Seo JT, Berridge MJ, Ciccolini F, Lipp P. *Calcium signalling—an overview. Seminars in Cell & Developmental Biology*. 2001; 12(1):3-10

Boyadjieva NI, Sarkar DK. Role of microglia in ethanol's apoptotic action on hypothalamic neuronal cells in primary cultures. *Alcoholism: Clinical and Experimental Research*. 2010, 34:1835-1842.

Breunig M, Lungwitz U, Liebl R, Goepferich A. Breaking up the correlation between efficacy and toxicity for nonviral gene delivery. *Proceeding of the National Academy of Sciences of the United States of America*. 2007; 104(36):14454–14459.

Burnstock G. Purinergic signalling: from discovery to current developments. *Experimental Physiology*. 2014; 99(1):16–34.

Burnstock G. Purinergic Signalling: Therapeutic Developments. *Frontiers in Pharmacology*. 2017; 661(8):5-13.

Burnstock G. Purinergic signalling. *British Journal of Pharmacology*. 2006; 147:172–181.

Burnstock G, Kennedy C**.** P2X receptors in health and disease**.** *Advances in Pharmacology*. 2011; 61:333-372.

Casati A, Frascoli M, Traggiai E, Proietti M, Schenk U, and Grassi F. Cell-autonomous regulation of hematopoietic stem cell cycling activity by ATP. *Cell Death and Differentiation.* 2011; 18:396-404.

Charlton SJ, Brown CA, Weisman GA, Turner JT, Erb L, Boarder MR. Cloned and transfected P2Y4 receptors: characterization of a suramin and PPADS-insensitive response to UTP. *British Journal of Pharmacology*. 1996; 119:1301-1303.

Chataigneau T, Lemoine D, Grutter T. Exploring the ATP-binding site of P2X receptors. *Frontiers in Cellular Neuroscience*. 2013; 7(273):273.

ChEBI. CHEBI:17295 - L-phenylalanine. Last Updated: 2019. Available at: https://www.ebi.ac.uk/chebi/searchId.do?chebiId=CHEBI:17295.

Cheng HP, Wei S, Wei LP, Verkhratsky A. *Calcium signaling in physiology and pathophysiology*. 2006; 27(2):767-772.

Clapham DE. Calcium Signalling, *Cell*. 2007; 131(6):1047-1058.

Coddou C, Sandoval R, Hevia MJ, Stojilkovic SS. Characterization of the antagonist actions of 5-BDBD at the rat P2X4 receptor. *Neuroscience Letters*. 2019; 690: 219-224.

Cragie E, Menzies RI, Larsen CK, Jacquillet G, Carrel M, Wildman SS, Loffing J, Leipziger J, Shirley DG, Bailey MA, Unwin RJ. The renal and blood pressure response to low sodium diet in P2X4 receptor knockout mice. *Physiological Report*. 2018; 6(20):13899.

Diaz-Hernandez JI, Gomez-Villafuertes R, Leon-Otegui M, Hontecillas-Prieto L, Del Puerto A, Trejo JL, Lucas JJ, Garrido JJ, Gualix J, Miras-Portugal MT. In vivo P2X7 inhibition reduces amyloid plaques in Alzheimer's disease through GSK3beta and secretases. *Neurobiology of Aging*. 2012; 33:1816-1828.

Di Virgilio F. Purinergic signalling between axons and microglia. *Novartis Foundation Symposia*. 2006; 276:253-258.

Di Virgilio F, Sarti AC, Falzoni S, De Marchi E, Adinolfi E. Extracellular ATP and P2 purinergic signalling in the tumour microenvironment. *Nature Reviews Cancer*. 2018; 18:601–618.

Dong Z, Saikumar P, Weinberg JM, Venkatachalam MA. Calcium in cell injury and death. *Annual Review of Pathology Mechanisms of Disease*. 2006; 1(1):405-434.

Ekoski E, Webb TE, Simon J, Tornquist K. Mechanisms of P2 receptor-evoked DNA synthesis in thyroid FRTL-5 cells. *Journal of Cellular Physiology*. 2001; 187(2):166-175.

Ennion S, Hagan S, Evans RJ. The role of positively charged amino acids in ATP recognition by human P2X1 receptors. *Journal of Biological Chemistry*. 2000; 275(38):29361-29367.

Evans RJ. Orthosteric and allosteric binding sites of P2X receptors. *European Biophysics Journal*. 2009, 38(3):319–327.

Evans RJ. Structural interpretation of P2X receptor mutagenesis studies on drug action. *British Journal of Pharmacology*. 2010; 161(5):961–97.

Evans RJ, Roberts AR. Cysteine substitution mutants give structural insight and identify ATP binding and activation sites at P2X receptors. *Journal of Neuroscience*. 2007; 27(15): 4072–4082.

Fan C, Zhao X, Guo X, Cao X, Cai J. P2X4 promotes interleukin-1β production in osteoarthritis via NLRP1. *Molecular Medicine Reports*. 2013; 9(1):340-344.

Fischer R, Grützmann R, Blasco HPJ, Kalthof B, Gadea PC, Stelte-Ludwig B, Woltering E, Wutke M: Benzofuro-1,4-diazepin-2-one derivatives. 2005; Patent Number: EP1608659A1.
Fong J. Hypocalcaemia. *Canadian Family Physician*. 2012; 58(2):158–162.

Fischer W, Franke H, Groger-Arndt H, Illies P. Evidence for the existence of P2Y1,2,4 receptor subtypes in HEK-293 cells: reactivation of P2Y1 receptors after repetitive agonist application. *Naunyn-Schmiedeberg's Archives of Pharmacology*. 2005; 371(6):466-472.

Grace PM, Rolan PE, Hutchinson MR. Peripheral immune contributions to the maintenance of central glial activation underlying neuropathic pain. *Brain, Behavior, and Immunity*. 2011; 25(7):1322-1332.

Garcia-Guzman M, Soto F, Gomez-Hernandez JM, Lund PE, Stuhmer W. Characterization of recombinant human $P2X_4$ receptor reveals pharmacological differences to the rat homologue. *Molecular Pharmacology*. 1997; 51:109–118.

Gofman L, Cenna JM, Potula R. P2X4 receptor regulates alcohol-induced responses in microglia. *Journal of Neuroimmune Pharmacology*. 2014; 9(5):668-678.

Halim NSSA, Fakiruddin KS, Ali SA, Yahaya BH. A Comparative Study of Non-Viral Gene Delivery Techniques to Human Adipose-Derived Mesenchymal Stem Cell. *International Journal of Molecular Sciences*. 2014; 15(9): 15044–15060.

Hattori M, Gouaux E. Molecular mechanism of ATP binding and ion channel activation in P2X receptors. *Nature.* 2012; 485:207–212.

He ML, Gonzalez-Iglesias AE, Stojilkovic SS. Role of nucleotide P2 receptors in calcium signalling and prolactin release in pituitary lactotrophs. *Journal of Biological Chemistry*. 2003; 276:46270-46277.

Hung SC, Choi CH, Said-Sadier N, Johnson L, Atanasova KR, Sellami H, Yilmaz O, Ojcius D M. P2X4 assembles with P2X7 and pannexin-1 in gingival epithelial cells and modulates ATP-induced reactive oxygen species production and inflammasome activation. *Plos One.* 2013; 8(7):e70210.

Jacobson KA, Jarvis MF, Williams M. Purine and pyrimidine (P2) receptors as drug targets. *Journal of Medicinal Chemistry*. 2002; 45:4057–4093.

Jacobson KA, Muller CE. Medicinal Chemistry of Adenosine, P2Y and P2X Receptors. *Neuropharmacology*. 2016; 104:31–49.

Jarvis MF. The neural-glial purinergic receptor ensemble in chronic pain states. *Trends in Neurosience*. 2010; 33(1):48-57.

Jiang R, Lemoine D, Martz A, Taly A, Gonin S, Prado de Carvalho L, Specht A, Grutter T. Agonist trapped in ATP-binding sites of the P2X2 receptor. *Proceedings of the National Academy of Sciences of the United States of America*. 2011; 108(22):9066-71.

Jiang R, Taly A, Lemoine D, Martz A, Specht A, Grutter T. Intermediate closed channel state(s) precede(s) activation in the ATP-gated P2X2 receptor. *Channels*. 2012; 6:398–402.

Jiang L-H, Fo R, Surprenant A, North RA. Identification of amino acid residues contributing to the ATP-binding site of a purinergic P2X receptor. *Journal of Biological Chemistry*. 2000; 275(44):34190–34196.

Jo YH, Donier E, Martinez A, Garret M, Toulmé E, Boué-Grabot E. *Journal of Biological Chemistry.* 2011; 286(22):19993-20004.

Jones CA, Chessell JP, Simon J, Barnard EA, Miller KJ, Michel AD, Humphrey PPA. Functional characterization of the $P2X_4$ receptor orthologues. *British Journal of Pharmacology*. 2000; 129(2):388–394.

Kaczmarek-Hájek K, LörinczíE, Hausmann R, and Nicke A. Molecular and functional properties of P2X receptors—recent progress and persisting challenges. *Purinergic Signalling*. 2012; 8(3):375–417.

Kannurpatti SS, Joshi PG, Joshi NB. Calcium sequestering ability of mitochondria modulates influx of calcium through glutamate receptor channel. *Neurochemical Research*. 2000; 25(12):1527-1536.

Kass GE, Orrenius S. Calcium signaling and cytotoxicity. *Environmental Health Perspectives*. 1999;107(1):25-35.

Kawate T, Michel JC, Birdsong WT, Gouaux E. Crystal structure of the ATP-gated P2X4 ion channel in the closed state. *Nature*. 2009; 30; 460(7255): 592–598.

Kim HJ, Ajit D, Peterson TS, Wang Y, Camden JM, Wood GW, Sun GY, Erb L, Petris Krzyszczyk P, Schloss R, Palmer A, Berthiaume F. The Role of Macrophages in Acute and Chronic Wound Healing and Interventions to Promote Pro-wound Healing Phenotypes. *Frontiers in Pharmacology*. 2018; 9:419.

Kumada T, Jiang Y, Cameron DB, Komuro H. How does alcohol impair neuronal migration? *Journal of Neuroscience Research*. 2007; 85(3):465-470.

Kwon, HJ. Extracellular ATP signaling via P2X4 receptor and cAMP/PKA signaling mediate ATP oscillations essential for prechondrogenic condensation. *Journal of Endocrinology.* 2012; 214(3):337-348.

Layhadi JA, Turner J, Crossman D, Fountain SJ. ATP Evokes Ca^{2+} Responses and CXCL5 Secretion via $P2X_4$ Receptor Activation in Human Monocyte Derived Macrophages. *The Journal of Immunology*. 2018; 200:1159-1168.

Ledderose C, Liu K, Kondo Y, Slubowski CJ, Dertnig T, Denicolo S, Arbab M, Hubner J, Konrad K, Fakhari M, Lederer JA, Robson SC, Visner GA, Junger WG. Purinergic P2X4 receptors and mitochondrial ATP production regulate T cell migration. *Journal of Clinical Investigation*. 2018; 128(8):3583-3594.

Li M, Silberberg SD, Swartz KJ. Subtype-specific control of P2X receptor channel signalling by ATP and Mg2+. *Proceedings of the National Academy of Sciences of the United States of America*. 2013; 110(36):3455-3463.

Linden J. Adenosine in tissue protection and tissue regeneration*. Molecular Pharmacology*. 2005; 67:1406–1413.

MacDermott AB, Henzi V, Reichling DB. Characterization of Glutamate Receptor Function Using Calcium Photometry and Imaging. *Methods in Neurosciences*. 1994; 19:283-303.

Marchand F, Perretti M, McMahon SB. Role of the immune system in chronic pain. *Nature Reviews Neuroscience*. 2005; 6(7):521-32.

Martinez NA, Ayala AM, Martinez M, Martinez-Riviera FJ, Miranda JD, Silva WI. Caveolin-1 Regulates the $P2Y_2$ Receptor Signalling in Human 1321N1 Astrocytoma Cells. *Journal of Biological Chemistry*. 2016; 291(23):12208–12222.

Marucci G, Lammini C, Buccioni M, Dal Ben D, Lamberducci C, Amantini C, Santonini G, Kandhavelu M, Abbracchio MP, Lecca D, Volpini R, Cristalli G. Comparison and optimization of transient transfection methods at human astrocytoma cell line 1321N1. *Analytical Biochemistry*. 2011; 414(2):300-302.

Marquez-Klaka B, Rettinger J, Bhargava Y, Eisele T, Nicke. Identification of an intersubunit cross-link between substituted cysteine residues located in the putative ATP binding site of the P2X1 receptor. *Journal of Neuroscience*. 2007; 27(6):1456-1466.

Masuda T, Ozono Y, Mikuriya S, Kohro Y, Tozaki-Saitoh H, Iwatsuki K*.* Dorsal horn neurons release extracellular ATP in a VNUT-dependent manner that underlies neuropathic pain. *Nature Communications*. 2016; 7:12529.

Maurisse R, De Semir D, Emamekhoo H, Bedayat B, Abdolmohammadi A, Parsi H, Gruenert DC. Comparative transfection of DNA into primary and transformed mammalian cells from different lineages**.** *BMC Biotechnology*. 2017; 10(9):1-10.

Neary JT, Rathbone MP, CatabenniI F, Abbrachio MP, Burnstock G. Trophic actions of extracellular nucleotides and nucleosides on glial and neuronal cells. *Trends in Neuroscience*. 1996; 19:13–18.

Nicke A, Baumert HG, Rettinger J, Eichele A, Lambrecht G, Mutschler E, Schmalzing G. P2X1 and P2X3 receptors form stable trimers: a novel structural motif of ligand-gated ion channels. *The EMBO Journal*. 1998; 17(11):3016–3028.

North RA. Molecular physiology of P2X receptors**.** *Physiology Review*. 2002; 82:1013-1067.

Lim JY, Park SH, Jeong CH, Oh JH, Kim SM, Ryu CH, Park SA, Ahn JG, Oh W, Jeun SS, Chang JW. Microporation is a valuable transfection method for efficient gene delivery into human umbilical cord blood-derived mesenchymal stem cells. BMC Biotechnology. 2010; 10:38.

Lin CH, Su CH, Hwang PP. Calcium-Sensing Receptor Mediates Ca^{2+} Homeostasis by Modulating Expression of PTH and Stanniocalcin. *Endocrinology*. 2014; 155(1):56-67.

Matsumura Y, Yamashita T, Sasaki A, Nakata E, Kohno K, Masuda T, Tozaki-Saitoh H, Imai T, Kuraishi Y, Tsuda M, Inoue K. A novel P2X4 receptor-selective antagonist produces anti-allodynic effect in a mouse model of herpetic pain. *Scientific Reports*. 2016; 6:32461.

Meng X, Cai C, Wu J, Cai S, Ye C, Chen H, Yang Z, Zeng H, Shen Q and Zou F. TRPM7 mediates breast cancer cell migration and invasion through the MAPK pathway. *Cancer Letters*. 2013; 333:96-102.

Mohammad MR, Ziyad TM, Muhammad J, Houjin Z. The Aromatic Stacking Interactions Between Proteins and their Macromolecular Ligands. *Current Protein and Peptide Science*. 2015; 16(6):502-512.

Nowycky MC, Thomas AP. Intracellular Calcium Signalling. *Journal of Cell Science*. 2002; 115:3715-3716.

Ohata Y., Ogata S., Nakanishi K., Kanazawa F., Uenoyama M., Hiroi S. Expression of P2X4R mRNA and protein in rats with hypobaric hypoxia-induced pulmonary hypertension. *Circulation Journal*. 2011; 75(4):945–954.

Paredes RM, Etzler JC, Watts LT, Lechleiter JD. Chemcal calcium indicators. *Methods*. 2008; 46(3):143–151.

Pinto MC, Kihara AH, Goulart VA, Tonelli FM, Gomes KN, Ulrich H, Resende RR. Calcium signaling and cell proliferation. *Cellular Signalling*. 2015; 27(11):2139-49.

Priel A, Silberberg SD. Mechanism of ivermectin facilitation of human P2X4 receptor channels. *Journal of General Physiology*. 2004; 123(3):281-293.

Pugilese AM, Trincavelli ML, Lecca D, Coppi E, Fumagalli M, Ferrario S, Faili P, Daniele S, Martini C, Pedata F, Abbracchio MP. Functional characterization of two isoforms of the P2Y-like receptor GPR17: [^{35}S]GTPγS binding and electrophysiological studies in 1321N1 cells. *American Journal of Physiology*. 2009; 297:1028–1040.

Qi Z, Mutase K, Obata S, Sokabe M. Extracellular ATP-dependent activation of plasma membrane Ca^{2+} pump in HEK-293 cells. *British Journal of Pharmacology*. 2000; 131(2): 370–374.

Ralevic V, Burnstock G. Receptors for purines and pyrimidines. *Pharmacology Review*. 1998; 50:413–492.

Roberts JA, Vial C, Digby H, Agboh K, Wen H, Atterbury-Thomas A, Evans R. Molecular properties of P2X receptors. *Pflügers Archive European Journal of Physiology*. 2006; 452(5):486–500.

Roberts JA, Evans RJ. ATP binding at human P2X1 receptors. Contribution of aromatic and basic amino acids revealed using mutagenesis and partial agonists. *Journal of Biological Chemistry*. 2004; 279:9043–9055.

Romanov RA, Khokhlov AA, Bystrova MF, Rogachevskaja OA, Yatzenka YE, Kolesnikov SS. Monitoring ATP release from individual cells with a biosensor. *Biochemistry (Moscow) Supplement Series A: Membrane and Cell Biology*. 2007; 1(3):240-245.

Schachter JB, Sromek SM, Nicholas RA, Harden TK. HEK293 human embryonic kidney cells endogenously express the P2Y1 and P2Y2 receptors. *Neuropharmacology*. 1997; 36(9):1181-1187.

Seye CI, Yu N, Gonzalez FA, Erb L, Weisman GA. The P2Y2 Nucleotide Receptor Mediates Vascular Cell Adhesion Molecule-1 Expression through Interaction with VEGF Receptor-2 (KDR/Flk-1). *Journal of Biological Chemistry*. 2004; 279(34):35679–35686.

Sigma Aldrich. 5-BDBD. Last Updated: 2019. Available at: https://www.sigmaaldrich.com/catalog/product/sigma/sml0450?lang=en&region=GB.

Sim JA, Chaumont S, Jo J, Ulmann L, Young MT, Cho K, Buell G, North RA, Rassendren F *Journal of Neuroscience*. 2006; 26(35):9006-9009.

Sim JA, Park CK, Oh SB, Evans RJ, North RA. P2X1 and P2X4 receptor currents in mouse macrophages. *British Journal of Pharmacology*. 2007; 152(8):1283-1290.

Sonnenfield T, Cronestrand R. Pharmacological vasodilation during reconstructive vascular surgery. *Acta Chirugica Scandinavica*. 1980; 146(1):9-14.

Soto F, Garcia Guzman M, Gomez-Hernandez JM, Hollman M, Karschin C, Stuhmer W. P2X4: an ATP-activated ionotropic receptor cloned from rat brain. Proceedings of the National Academy of Sciences of the United States of America. 1996; 93(8):3684-3688

Soto F, Lambrecht G, Nickel P, Stühmer W, Busch AE. Antagonistic properties of the suramin analogue NF023 at heterologously expressed P2X receptors. *Neuropharmacology*. 1999; 38(1):141-149.

Stelmashenko O, Lalo U, Yang Y, Bragg L, North RA, Compan V. Activation of trimeric P2X2 receptors by fewer than three ATP molecules. *Molecular Pharmacology*. 2012; 82:760–766.

Stokes L, Scurrah K, Ellis JA, Cromer BA, Skarratt KK, Gu BJ. A loss-of-function polymorphism in the human P2X4 receptor is associated with increased pulse pressure. *Hypertension*. 2011; 58:1086-1092.

Stokes L, Layhadi JA, Bibic L, Dhuna K, Fountain SJ. P2X4 Receptor Function in the Nervous System and Current Breakthroughs in Pharmacology. *Fronteirs in Pharmacology*. 2017; 8:291.

Tanyeli O, Duman I, Dereli Y, Gormus N, Toy H, Sahin AS. Relaxation matters: comparison of in-vitro vasodilatory role of botulinum toxin-A and papaverine in human radial artery grafts. *Journal of CardiothoracicSurgery*. 2019; 14(15):1-9.

Tharmalingham T, Ghebeh H, Wuerz T, Butler M. Pluronic enhances the robustness and reduces the cell attachment of mammalian cells. Molecular Biotechnology. 2008; 39(2):167-177.

Thibault K, Lin WK, Rancillac A, Fan M, Snollaerts T, Sordoillet V. BDNF-dependent plasticity induced by peripheral inflammation in the primary sensory and the cingulate cortex triggers cold allodynia and reveals a major role for endogenous BDNF as a tuner of the affective aspect of pain. *Journal of Neuroscience*. 2014; 34:14739-14751.

Tocris. 5-BDBD. Last updated: 2019. Available at: https://www.tocris.com/products/5-bdbd_3579.

Trang T, Salter M. P2X4 purinoceptor signalling in chronic pain. *Purinergic Signalling*. 2012; 8(3):621-8.

Toulme E, Garcia A, Samways D, Egan TM, Carson MJ, Khakh BS. P2X4 receptors in activated C8–B4 cells of cerebellar microglial origin. *The Journal of General Physiology*. 2010; 135:333-353.

Tsuda M, Shigemoto-Mogami Y, Koizumi S, Mizokoshi A, Kohsaka S, Salter MW, Inoue K. P2X4 receptors induced in spinal microglia gate tactile allodynia after nerve injury. *Nature*. 2003; 424(6950):778-783.

Tsuda M, Inoue K, Koizumi S. ATP- and Adenosine-Mediated Signalling in the Central Nervous System: Chronic Pain and Microglia: Involvement of the ATP Receptor $P2X_4$. *Journal of Pharmacological Sciences*. 2004; 94(2):112-114.

Ulmann L, Hatcher JP, Hughes JP, Chaumont S, Green PJ, Conquet F, Buell GN, Reeve AJ, Chessell IP, Rassendren F. Up-regulation of P2X4 receptors in spinal microglia after peripheral nerve injury mediates BDNF release and neuropathic pain. *Journal of Neuroscience*. 2008; 28:11263–11268.

Vavra V, Bhattacharya A, Zemkova H. Facilitation of glutamate and GABA release by P2X receptor activation in supraoptic neurons from freshly isolated rat brain slices. *Neuroscience.* 2011; 188(0):1-12.

Velasquez S, Eugenin EA. Role of Pannexin-1 hemichannels and purinergic receptors in the pathogenesis of human diseases. *Fronteirs in Physiology*. 2014; 96(5): 1-12**.**

Volonté C, D'Ambrosi N. Membrane compartments and purinergic signalling: the purinome, a complex interplay among ligands, degrading enzymes, receptors and transporters. *FEBS Journal*. 2009; 276:318-332.

Wang J, Yu Y. Insights into the channel gating of P2X receptors from structures, dynamics and small molecules. *Acta Pharmacologica Sinica*. 2016; 37(1):44–55.

Wang T, Larcher LM, Ma L, Veedu RN. Systematic Screening of Commonly Used Commercial Transfection Reagents towards Efficient Transfection of Single-Stranded Oligonucleotides. *Molecules*. 2018; 23(10):2564.

Watkins LR, Milligan ED, Maier SF. Glial activation: a driving force for pathological pain. *Trends in Neuroscience*. 2001; 24(8):450-455.

Waxham MN. Neurotransmitter receptors. *Fundamental Neuroscience*. 2013; 4:163-187.

Wheeler SE, Bloom JW. Toward a more complete understanding of noncovalent interactions involving aromatic rings. *Journal of Physical Chemistry*.2014; 118(32):6133-6147.

Wilkinson WJ, Jiang LH, Surprenant A, North RA. Role of ectodomain lysines in the subunits of the heteromeric P2X2/3 receptor. *Molecular Pharmacology*. 2006; 70(4):1159-63.

Wu T, Dai M, Shi XR, Jiang ZG, and Nuttall AL. Functional expression of P2X4 receptor in capillary endothelial cells of the cochlear spiral ligament and its role in regulating the capillary diameter. *American Journal of Physiology-Heart and Circulatory Physiology*. 2011; 301:H69-78.

Wyatt LR, Finn DA, Khoja S, Yardley MM, Asatryan L, Alkana RL. Contribution of P2X4 receptors to ethanol intake in male C57BL/6 mice. *Neurochemical Research*. 2014; 39:1127-1139.

Yamano S, Dai J, Moursi AM. Comparison of transfection efficiency of nonviral gene transfer reagents. *Molecular Biotechnology*. 2010; 46(3):287-300.

Yang A, Sonin D, Jones L, Barry WH, Liang BT. A beneficial role of cardiac P2X4 receptors in heart failure: rescue of the calsequestrin overexpression model of cardiomyopathy. *American Journal of Physiology*. 2004; 287:1096-1103.

Yang R, Beqiri D, Shen JB, Redden JM, Dodge-Kafka K, Jacobson KA, Liang BT. P2X4 receptor–eNOS signalling pathway in cardiac myocytes as a novel protective mechanism in heart failure. *Computational and Structural Biotechnology Journal*. 2015; 13:1–7.

Yang R, Liang BT. Cardiac $P2X_4$ Receptors, Targets in Ischemia and Heart Failure. *Circulation Research*. 2012; 111(4): 397–401.

Young M. P2X receptors: dawn of the post-structure era. Trends in Biochemical Sciences. 2010; 35(2):83-90.

Yu W, Hill WG, Robson SC, Zeidel ML. Role of P2X4 Receptor in Mouse Voiding Function. *Nature Scientific Reports*. 2018; 8:1838.

Zimmermann M. Pathobiology of neuropathic pain. *European Journal of Pharmacology*. 2001; 429:23–37.